Quarterly Reviews of Biophysics **37**, 3/4 (2004), pp. 285–314. © 2004 Cambridge University Press
doi:10.1017/S003358350500404X Printed in the United Kingdom

Role of cofactors in metalloprotein folding

Corey J. Wilson[1,2], David Apiyo[1] and Pernilla Wittung-Stafshede[1,2,3]*

[1] Department of Biochemistry and Cell Biology, Rice University, Houston, TX, USA
[2] Keck Center for Structural Computational Biology, Rice University, Houston, TX, USA
[3] Department of Chemistry, Rice University, Houston, TX, USA

Abstract. Metals are commonly found as natural constituents of proteins. Since many such metals can interact specifically with their corresponding unfolded proteins *in vitro*, cofactor-binding prior to polypeptide folding may be a biological path to active metalloproteins. By interacting with the unfolded polypeptide, the metal may create local structure that initiates and directs the polypeptide-folding process. Here, we review recent literature that addresses the involvement of metals in protein-folding reactions *in vitro*. To date, the best characterized systems are simple one such as blue-copper proteins, heme-binding proteins, iron-sulfur-cluster proteins and synthetic metallopeptides. Taken together, the available data demonstrates that metals can play diverse roles: it is clear that many cofactors bind before polypeptide folding and influence the reaction; yet, some do not bind until a well-structured active site is formed. The significance of characterizing the effects of metals on protein conformational changes is underscored by the many human diseases that are directly linked to anomalous protein–metal interactions.

* Author for correspondence: P. Wittung-Stafshede, Biochemistry and Cell Biology, MS-140, Rice University, 6100 Main Street, Houston, TX 77251, USA.
Tel.: 713-348-4076; Fax: 713-3485154; E-mail: pernilla@rice.edu

1. Metals in proteins

Although traditionally regarded as organic, life is inorganic too. At present, we are aware of 13 metals which are essential for plants and animals (Bertini *et al.* 1994; Lippard & Berg, 1994). Four of these, sodium, potassium, magnesium and calcium, are present in large quantities and are known as bulk metals (Fenton, 1995). The remaining nine, which are present in small quantities, are the d-block elements vanadium, chromium, molybdenum, manganese, iron, cobalt, nickel, copper and zinc, and are known as the trace metals. The bulk metals form 1–2% of the human body-weight whereas the trace elements represent less than 0·01%. Even of iron, the most widely used trace metal, we need only of the order of 4–5 g in a human body (Fenton, 1995). The concentrations of metals in the cells are strictly regulated at their respective optimum levels: too much or too little is often harmful and may even be lethal to the organism. Most of the trace metals are found as natural constituents of proteins. In this way, Nature has taken advantage of the special properties of the metal ions and tuned them by protein encapsulation to perform a wide variety of specific functions associated with life processes (Bertini *et al.* 1994; Lippard & Berg, 1994).

More than 30% of all proteins in the cells exploit one or more metals to perform their specific functions (Gray, 2003); over 40% of all enzymes contain metals (Bertini *et al.* 1994; Lippard & Berg, 1994). The amino acids that regularly act as metal ligands in proteins are thiolates of cysteines, imidazoles of histidines, carboxylates of glutamic and aspartic acids, and phenolates of tyrosines. Each metal is considered a Lewis acid and favors different sets of protein ligands; the preferences are frequently dictated by the hard-soft theory of acids and bases. The coordination number and geometry of each metal site is determined by the metal's oxidation state albeit substantial distortions from the idealized structures can and do occur in metalloproteins (Bertini *et al.* 1994; Lippard & Berg, 1994). Due to the unique chemical properties of each metal, different metals are apt for different types of biological functions, although there is overlap is some cases.

In Fig. 1, we have summarized various classes of metal-binding proteins. Iron and copper are redox-active metals (i.e. can switch between oxidized and reduced forms: Cu^{2+}/Cu^{1+} and Fe^{3+}/Fe^{2+}) and often participate in electron transfer (Fenton, 1995). In respiration and photosynthesis processes, small redox-active metalloproteins facilitate electron-transfer reactions by alternately binding to specific integral membrane proteins that often contain several metal sites. Well-known examples of soluble redox-active metalloproteins are iron-sulfur (Fe-S) cluster proteins, heme-binding cytochromes and blue-copper proteins. Iron and copper are also involved in dioxygen (O_2) storage and carriage via metalloproteins [e.g. hemoglobin, myoglobin (Mb) and hemocyanin]. Furthermore, iron storage as well as iron and copper transfer are facilitated in the cells by specific proteins. In contrast to iron and copper, zinc serves as a superacid center in several metalloenzymes, promoting hydrolysis or cleavage of a variety of chemical bonds. Representative proteins that use catalytic zinc ions are carboxypeptidases, carbonic anhydrase, and alcohol dehydrogenase. In addition, zinc ions often play structural roles in proteins [e.g. in superoxide dismutase (SOD) and zinc-finger motifs]. Most of the other trace metals have been identified as parts of metalloenzymes (Lippard & Berg, 1994; Gray, 2003). For example, manganese is found as a cofactor in mitochondrial SOD, inorganic phosphatase and photosynthesis system II. Nickel functions in enzymes such as urease and several hydrogenases. Both molybdenum and vanadium are found in nitrogenases, where they are present in larger clusters containing also iron and sulfur ions (Fenton, 1995).

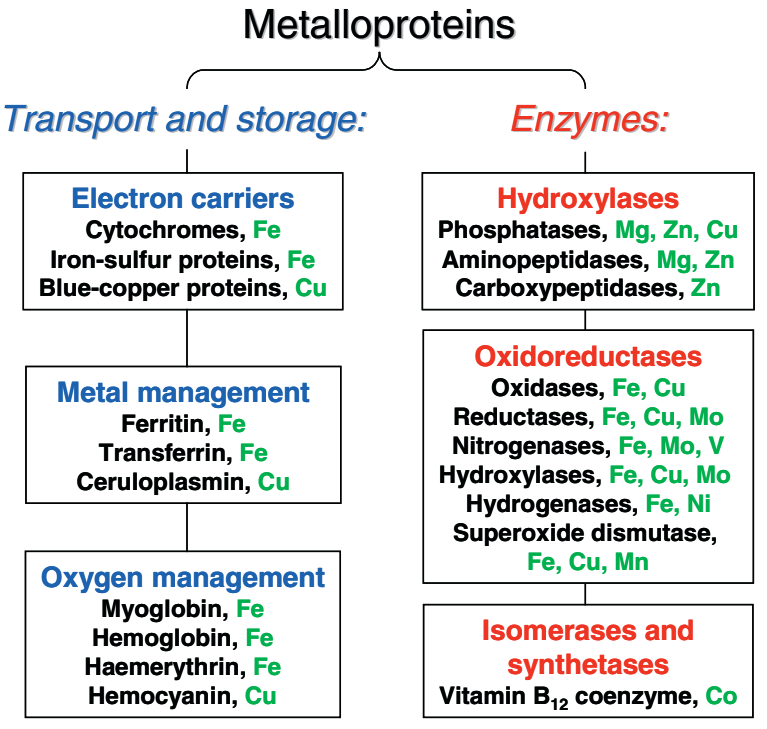

Fig. 1. Classification of metalloproteins (Fenton, 1995) into different groups according to their functions. Metal cofactors in each group of protein are highlighted in green.

Owing to the advances in crystallography, time-resolved spectroscopic methods and protein engineering since the 1970s, we now have high-resolution structures of many metalloproteins and know a great deal about their mechanisms of action (Gray, 2003). Despite this wealth of information, the folding pathways for metalloproteins are mostly unknown (Wittung-Stafshede, 2002).

2. Protein folding and metals

To function, polypeptides (released from the ribosome *in vivo* or denatured *in vitro*) must fold into their unique three-dimensional protein structures. Many proteins fold spontaneously *in vitro*, although the mechanisms are not entirely understood on a molecular level. Small, single-domain proteins (<100 residues), lacking both disulfide bonds and proline isomerization, often fold by two-state equilibrium and kinetic mechanisms (Jackson, 1998; Kamagata *et al.* 2004). For such proteins, three states are important for defining kinetic and thermodynamic behavior: the native, transition and denatured states. The transition state consists of a set of structures (i.e. the transition-state ensemble) whose formation is rate-limiting for folding of the native state from the denatured ensemble. As the transition state never accumulates, details about its properties must be inferred indirectly (Lindorff-Larsen *et al.* 2004). The protein engineering approach, termed phi (ϕ) value analysis, has proved to be the most important experimental strategy for obtaining specific information about interactions between residues in the transition state (Matouschek *et al.* 1990; Matouschek & Fersht, 1991).

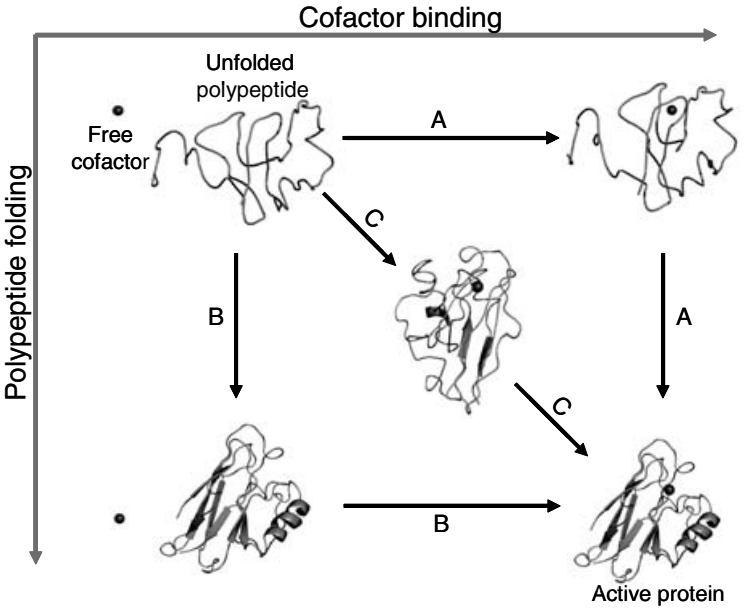

Fig. 2. The scheme shows three possible pathways for folding and assembly of an active metal-binding protein. The cofactor may bind before polypeptide folding (path A), after complete protein folding (path B), or to a partially folded protein structure (path C).

Correlations of experimental folding rates for small two-state folding proteins (lacking cofactors) have been studied against several parameters (e.g. thermodynamic stability, polypeptide-chain length, transition-state placement, and native-state topology). Interestingly, the relative contact order, reporting on the degree of local *versus* non-local contacts in the native state, was found to be the most statistically significant parameter (Plaxco *et al.* 1998, 2000). This correlation is supported by both experimental and theoretical evidence and highlights the importance of native-state topology, as opposed to fine details of the polypeptide sequence, as a determinant of protein-folding rates (Plaxco *et al.* 1998, 2000; Fersht, 2000; Makarov & Plaxco, 2003; Chavez *et al.* 2004). In addition to the native, transition, and unfolded states, proteins longer than 100 residues often populate conformations, either transiently or at equilibrium, which display mixed properties of the native and denatured states. In such cases, populated intermediates are evident in the equilibrium- and/or kinetic-folding reactions; thus, the mechanisms deviate from simple two-state (Matthews, 1993; Roder & Colon, 1997; Sanchez & Kiefhaber, 2003). Folding intermediates may be on-pathway (i.e. facilitating the reaction) or off-pathway (i.e. acting as traps that may lead to aggregation) or multiple pathways may be present in which different intermediates coexist (States *et al.* 1987; Privalov, 1996; Fersht, 1999).

Metal-binding proteins fold in a cellular environment where their cognate cofactors are present, either free in the cytoplasm or bound to delivery proteins. Thus, the question arises as to when metals bind to their corresponding proteins: specifically, do they bind before, during or after polypeptide folding? As demonstrated *in vitro*, many metalloproteins (e.g. cytochrome b_{562}, Mb, azurin, and the Cu_A domain) retain strong metalloligand binding after polypeptide unfolding (Bertini *et al.* 1997; Robinson *et al.* 1997; Wittung-Stafshede *et al.* 1998a, b, 1999). This implies that *in vivo* metals may interact with their corresponding proteins before polypeptide folding takes place which could impact the folding reaction (Fig. 2). Local and non-local structure in the

unfolded protein may form due to specific coordination of the cofactor (Pozdnyakova *et al.* 2000). Such structural restriction of the ensemble of conformations may dramatically decrease the entropy of the unfolded state, limiting the conformational search for the native state (Luisi *et al.* 1999). The metal may this way serve as a nucleation site that directs polypeptide folding along a specific pathway in the free-energy landscape.

Notwithstanding the essential role of cofactors in proteins (Lippard & Berg, 1994), many metals are toxic when free in biological fluids and a number of diseases (e.g. Menke's syndrome and Wilson's disease) have been linked to alterations in cofactor–protein interactions (Rae *et al.* 1999). This underscores the fundamental importance of revealing the physical principles for metal interactions with folded, unfolded, and intermediate states of polypeptides. Here, we present a contemporary view of how metals influence protein-folding reactions. Important questions that we address are: Can metals bind to unfolded polypeptides? If so, what is the binding-site and affinity? Does a metal bound to an unfolded polypeptide affect the folding reaction? If a metal does not bind to the unfolded polypeptide, when during folding does it bind? What are the energetic and structural effects on the folded protein caused by the bound metal?

3. Blue-copper proteins

Blue-copper proteins (also called cupredoxins) are an important class of metalloproteins that carry out electron-transfer reactions (Lippard & Berg, 1994). The name comes from their intense blue absorption around 630 nm, which is a result of unique copper coordination. The best characterized blue-copper protein with respect to the role of metals in folding is *Pseudomonas aeruginosa* azurin. This is a small (128 residues) protein that is believed to facilitate electron transfer in denitrification/respiration chains (Adman, 1991). In recent years, it was proposed that the physiological function of azurin in *P. aeruginosa* involves electron transfer directly related to the cellular response to oxidative stress (Vijgenboom *et al.* 1997). Notably, in 2002 *P. aeruginosa* azurin was demonstrated to interact with the tumor-suppressor gene product p53 and act as an anti-cancer agent in cell-culture studies (Yamada *et al.* 2002). Thus, not only is *P. aeruginosa* azurin an excellent model, it is also a putative cancer-drug candidate.

Azurin has one α-helix and eight β-strands that fold into a β-barrel structure arranged in a double-wound Greek-key topology (Adman, 1991; Nar *et al.* 1992b) (Fig. 3). In *P. aeruginosa* azurin, the redox-active copper (Cu^{1+}/Cu^{2+}) is coordinated by two histidine imidazoles (His46 and His117), one cysteine thiolate (Cys112), and two weaker axial ligands, sulfur of methionine (Met121) and carbonyl of glycine (Gly45) in a trigonal bipyramidal geometry. It has been suggested that the polypeptide fold defines the exact geometry of the metal site, leading to the unusual Cu^{2+} coordination in azurin as well as in other blue-copper proteins (Wittung-Stafshede *et al.* 1998a). *In vitro*, *P. aeruginosa* azurin can bind many different metals in the active site (e.g. zinc). Crystal structures of apo- and holo-azurin [apo = without cofactor; holo = with cofactor] have shown that the overall three-dimensional structure is identical with and without a metal (copper or zinc) cofactor (Nar *et al.* 1991, 1992a, b). Since the zinc form of azurin is always a by-product upon azurin over-expression in *Escherichia coli*, and both copper and zinc may be present in the cells where the azurin polypeptide is produced, we have also addressed the role of zinc in the folding of azurin. Zinc is redox inactive and, therefore, more quantitative studies can be performed on zinc-azurin than on the copper form.

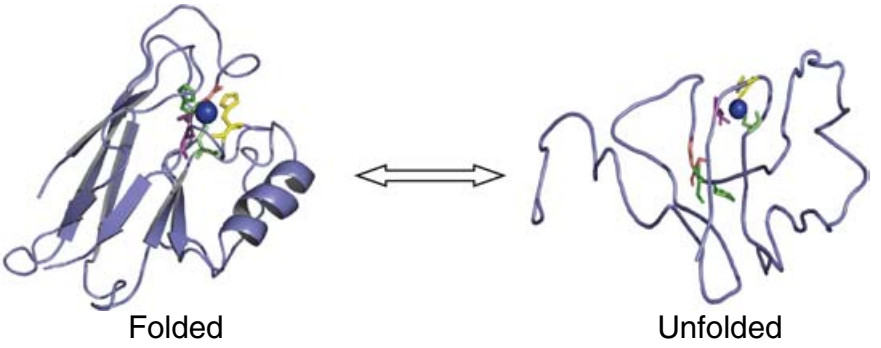

Fig. 3. Illustration of folded azurin (1AZU) with the five native-state copper ligands in stick representations (Gly45, pink; His46; green; His117, yellow; Cys112, light green; Met121, purple) and copper with blue fill. The representation of unfolded copper-azurin highlights the three residues that were found to coordinate copper in the unfolded state (His117, Cys112, Met121).

Early equilibrium-unfolding experiments (using the chemical denaturant guanidine hydrochloride, GuHCl) of oxidized (Cu^{2+}) and reduced (Cu^{1+}) azurin showed that the oxidized form is more stable than the reduced form. The unfolding curves were reversible and exhibited no protein-concentration dependence. This implied that the metal remained bound to the unfolded state, otherwise higher protein concentrations should have resulted in unfolding curves shifted to higher GuHCl concentrations (Leckner *et al.* 1997b). Different modes of spectroscopic detection yielded identical unfolding curves, in accord with two-state equilibrium-unfolding transitions. Based on the difference in thermodynamic stability for the two redox forms, we predicted that the copper in unfolded azurin has a reduction potential 0·13 V higher than that in folded azurin (Leckner *et al.* 1997a); subsequent cyclic-voltammetry experiments confirmed this prediction (20 °C, pH 7) (Wittung-Stafshede *et al.* 1998a). The high reduction potential for the unfolded state was rationalized by a trigonal metal-coordination that favored the Cu^{1+} form. This observation also implied that Cys112 remained a copper ligand in the unfolded-state complex (Wittung-Stafshede *et al.* 1998a). Equilibrium-unfolding studies of zinc-loaded azurin revealed that zinc, like copper, stayed bound to the polypeptide upon unfolding (Leckner *et al.* 1997b; Marks *et al.* 2004).

Subsequently, extended X-ray absorption fine structure (EXAFS) experiments in high GuHCl concentrations established that copper (Cu^{1+}) in unfolded azurin is coordinated in a trigonal geometry to one thiolate (i.e. Cys112), one histidine imidazole, and a third unknown ligand (DeBeer *et al.* 2000). To elucidate which one of the two native-state histidine ligands (i.e. His117 or His46) is involved in copper coordination in unfolded azurin, we prepared two single-site azurin variants (histidine-to-glycine mutations): His117Gly and His46Gly azurin (Pozdnyakova *et al.* 2001b). The results from equilibrium-unfolding experiments with these proteins strongly indicated that His117 is the histidine coordinating copper in unfolded azurin. Of the five native-state copper-ligands in azurin, three (Cys112, His117 and Met121) are situated in a loop region towards the C-terminus of azurin's polypeptide. Since two of these ligands had been confirmed as copper-ligands in the unfolded state, we suspected that Met121 may be the third ligand. To address this, we prepared the single-site mutant Met121Ala azurin (Marks *et al.* 2004). We found that Cu^{2+} dissociated from Met121Ala azurin early on in the polypeptide-unfolding reaction, suggesting that Met121 is indeed important for copper retention in the unfolded copper form of wild-type azurin. Notably, the equilibrium-unfolding behavior of the zinc form of Met121Ala

azurin was identical to that of wild-type azurin loaded with zinc, implying that zinc does not include Met121 as an unfolded-state ligand (Marks *et al.* 2004).

Complementary evidence for the copper and zinc ligands in unfolded azurin came from model peptide studies. We prepared a 13-residue peptide corresponding to the loop region in azurin (residues 111–123) that contains Cys112, His117 and Met121. This peptide was found to bind copper strongly, in a 1:1 stoichiometry (Pozdnyakova *et al.* 2000). Upon Cu^{2+} binding to the peptide, visible absorption bands appeared at 330 and 530 nm and β-like secondary structure formed. The presence of absorption at these wavelengths suggests thiolate(s) to Cu^{2+} ligand-to-metal charge transfer transitions (Mandal *et al.* 1997). Cu^{2+} binding to the peptide was also observed using isothermal titration calorimetry (ITC) although no thermodynamic parameters could be derived due to oxidation side reactions between Cu^{2+} and the peptide cysteine (Marks *et al.* 2004). Likewise, zinc also bound to the peptide in a 1:1 ratio as detected by ITC experiments; however, no secondary structure was induced when this complex formed. Metal titrations using ITC to a set of single point-mutated peptides, in which Cys112, His117 and Met121 were replaced individually by glycine, confirmed that all three ligands are required for copper binding (Fig. 3), whereas only Cys112 and His117 are needed for zinc binding (Marks *et al.* 2004).

Several studies have reported that apo, Cu^{1+}, Cu^{2+}, and Zn^{2+} forms of azurin unfold in two-state equilibrium reactions (pH 7, 20 °C) (Leckner *et al.* 1997b; Pozdnyakova *et al.* 2002; Pozdnyakova & Wittung-Stafshede, 2003). In the case of both copper and zinc, the metal stays bound upon unfolding, and the net effect on azurin's stability (compared to the stability of apo-azurin) corresponds to the difference in metal-affinity for the folded and unfolded polypeptide. The metals greatly stabilize native azurin; zinc, Cu^{1+}, and Cu^{2+} forms of azurin have thermodynamic stabilities of 39, 40, and 52 kJ mol^{-1} respectively whereas the stability of apo-azurin is 29 kJ mol^{-1} (pH 7, 20 °C) (Leckner *et al.* 1997b; Pozdnyakova *et al.* 2002; Pozdnyakova & Wittung-Stafshede, 2003). Using thermodynamic cycles coupling metal binding, protein stabilities and Cu^{2+}/Cu^{1+} reduction potentials, metal affinities for folded and unfolded forms of azurin could be estimated (Marks *et al.* 2004), Remarkably, the metal-affinity for the unfolded polypeptide is $\sim$17 000-fold higher for Cu^{2+} than for zinc. This increase in affinity may in part be explained by stabilization from the Met121 coordination with respect to copper, but not in the case of zinc. The analysis also shows that Cu^{1+} binds stronger to both folded and unfolded azurin compared to Cu^{2+}. This is consistent with the higher reduction potentials for the Cu^{2+}/Cu^{1+} pair when bound to the folded and unfolded polypeptides (i.e. 320 and 456 mV *versus* normal hydrogen electrode (NHE) respectively) compared to copper in aqueous solution (i.e. 150 mV *versus* NHE) (Wittung-Stafshede *et al.* 1998a).

To address possible pathways for formation of *active* azurin (i.e. folded protein with copper in the active site) *in vivo*, the time-scales for the two extreme scenarios (Fig. 4), copper binding before polypeptide folding (Pathway 1) and copper-binding after polypeptide folding (Pathway 2), were investigated. The folding and unfolding kinetics for apo-azurin follows two-state behavior (Pozdnyakova *et al.* 2001a, 2002; Pozdnyakova & Wittung-Stafshede, 2001a, b, 2003). The extrapolated folding time in water ($\tau \sim 7$ ms) is in good agreement with the speed predicted based on the topology-based contact order correlation mentioned in Section 2 (Pozdnyakova *et al.* 2002). Copper uptake by folded apo-azurin, which governs active protein through Pathway 2, is very slow (i.e. $\tau \sim 14$ min depending on protein-to-copper excess). Thus, Pathway 2 (Fig. 4) is limited by slow copper incorporation to folded apo-azurin (Pozdnyakova & Wittung-Stafshede, 2001a, b).

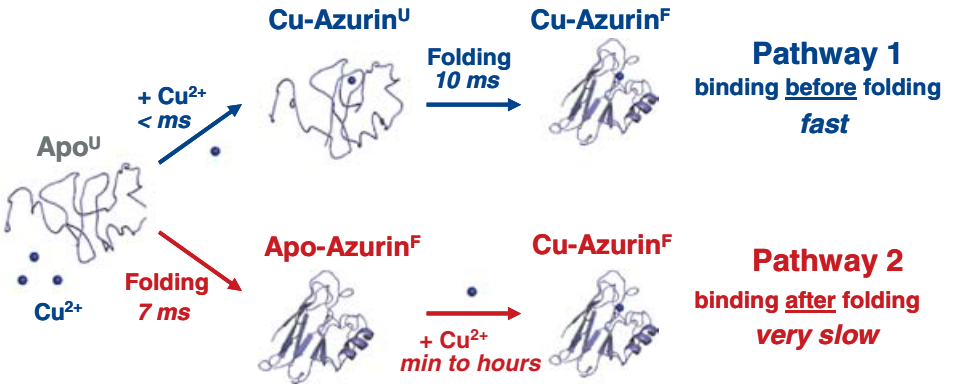

Fig. 4. Time-scales for formation of active azurin via Pathway 1 (cofactor-binding before polypeptide folding; blue) and Pathway 2 (polypeptide folding prior to cofactor binding; red) (pH 7, 20 °C). For each step, the approximate time is given. Upon comparison, Pathway 1 is four orders of magnitude faster than Pathway 2 (i.e. ms *versus* minutes–hours).

In contrast, we found the formation of active azurin to be much faster when copper is allowed to interact with the unfolded polypeptide. Active azurin forms in two kinetic phases with folding times extrapolated to water of $\tau \sim 10$ ms (major phase, 85% of molecules) and $\tau \sim 200$ ms (minor phase, 15% of molecules) (Pozdnyakova & Wittung-Stafshede, 2001a, b). Correlating copper-binding studies with the small model peptide supported that initial cofactor binding is fast and not rate-limiting. Therefore, in these latter experiments, active azurin formation follows Pathway 1 (Fig. 4), with rapid copper uptake before polypeptide folding. Taken together, introducing copper prior to protein folding results in much faster (>4000-fold) formation of *active* azurin (i.e. the folded holo-form) (Pozdnyakova & Wittung-Stafshede, 2001a, b).

Time-resolved folding and unfolding experiments with zinc-substituted azurin revealed that unfolding is a single-exponential process, whereas refolding is best fitted with double-exponential functions. The faster phase corresponds to 80% of the amplitude change and the slower phase to the remaining 20% at all denaturant conditions studied (Pozdnyakova & Wittung-Stafshede, 2003). We established that the bi-phasic behavior is due to the unfolded state of zinc-substituted azurin being heterogeneous (Pozdnyakova & Wittung-Stafshede, 2003). Since refolding of azurin in presence of copper was also bi-exponential, as was copper binding to the model peptide, it appears as if metals can bind to the unfolded azurin polypeptide in at least two ways. Metal coordination in the major population of unfolded molecules may include Cys112, His117 and Met121 for copper (Cys112 and His117 for zinc), resulting in the faster refolding rates. In the minor population of unfolded molecules, one of these ligands may be replaced by another residue or a solvent ion, resulting in retardation of polypeptide refolding (Pozdnyakova & Wittung-Stafshede, 2003).

In contrast to apo-azurin, the semi-logarithmic plot of zinc-azurin folding and unfolding rate constants *versus* denaturant concentration exhibits pronounced curvature in both folding and unfolding arms (Pozdnyakova & Wittung-Stafshede, 2003). In general, such behavior can be caused by transient aggregation, burst-phase intermediates and by movement of the transition-state placement. In pioneering work, Oliveberg and colleagues showed that the symmetrical curvature in the Chevron plot for the protein U1A was the result of transition-state movement (Oliveberg *et al.* 1998; Otzen *et al.* 1999; Ternstrom *et al.* 1999; Oliveberg, 2001). In the case of

zinc-substituted azurin, we could also assign the curvature to movement of the transition state as a function of denaturant concentration. At low concentrations of denaturant the transition state occurs early in the folding reaction, whereas at high denaturant concentration it moves closer to the native structure. Taking into account the curvature, the folding time in water is $\sim$20 ms for the major population of zinc-substituted azurin (Pozdnyakova & Wittung-Stafshede, 2003). Upon neglecting the minor slower phase, refolding of zinc-bound azurin proceeds in a two-state reaction with roughly the same polypeptide-folding speed in water as apo- and copper-bound azurin. In fact, extrapolated folding rates in water for apo-azurin, two point-mutated apo-azurin forms, zinc-substituted azurin (major phase), and azurin in presence of excess of copper (major phase) all fall within the range of 50–150 s^{-1} (Pozdnyakova & Wittung-Stafshede, 2003). Since the thermodynamic stability of these species ranges between 19–52 kJ mol^{-1}, the *native-state topology*, and not thermodynamic stability or the presence of cofactor interactions, appears to be the major determinant of the folding speed in water.

We recently characterized apo-azurin's folding-transition state using ϕ-value analysis (Wilson & Wittung-Stafshede, 2005a). The focus was on a set of core residues found to be structural determinants in 94% of all sandwich-like proteins (Kister *et al.* 2002). Apo-azurin's folding nucleus appears highly polarized; three core residues (Val31, Leu33 and Leu50) have ϕ-values of 1 (e.g. native-like structure in the transition state) whereas other residues have close-to-zero (e.g. unfolded-like environment in the transition state) ϕ-values (Wilson & Wittung-Stafshede, 2005a). In a study of a Cy112Ser variant of apo-azurin, another group also confirmed the importance of Val31, Leu33 and Leu50 in the folding-transition state (Engman *et al.* 2004). In sharp contrast to apo-azurin, ϕ-value analysis of zinc-substituted azurin's moving folding nucleus demonstrates that it is delocalized throughout the protein and gradually grows more native-like around a leading density centered in the core (Wilson & Wittung-Stafshede, 2005b). The dramatic difference in apparent kinetic behavior for the two forms of azurin can be rationalized as a minor alteration on a *common* free-energy profile that exhibits a broad activation barrier. The fixed transition state for apo-azurin may be the result of a small pointed feature projecting from the top of an otherwise broad free-energy profile. The presence of zinc in the unfolded state suppresses this local bump and the broad activation barrier becomes accessible.

4. Heme-binding proteins

c-Type cytochromes, characterized by covalent attachment of a iron-porphyrin at two cysteine residues, are proteins implicated in electron-transfer processes in both eukaryotic and prokaryotic organisms (Scott & Mauk, 1996). Although the transfer of electrons is always achieved by passing from the oxidized to the reduced form of the iron in the heme, there is nevertheless a great deal of diversity in the sequence and three-dimensional structure of these proteins which are classified into four types (see Scott & Mauk, 1996). The type-1 cytochromes *c* comprises the largest group and includes mitochondrial cytochrome *c* and bacterial cytochrome c_2 among others. They are usually small, soluble proteins with helical structures (Fig. 5). The single heme is covalently attached near the N-terminus, with histidine as the fifth ligand and methionine as the sixth ligand to the iron (Scott & Mauk, 1996).

The folding kinetics of *c*-type cytochrome proteins has been extensively studied (Hagen *et al.* 1996; Mines *et al.* 1996; Colon *et al.* 1997; Pierce & Nall, 1997; Yeh *et al.* 1997; Hammack *et al.* 1998; Bai, 1999; Chen *et al.* 1999; Telford *et al.* 1999; Yeh & Rousseau, 2000; Wittung-Stafshede,

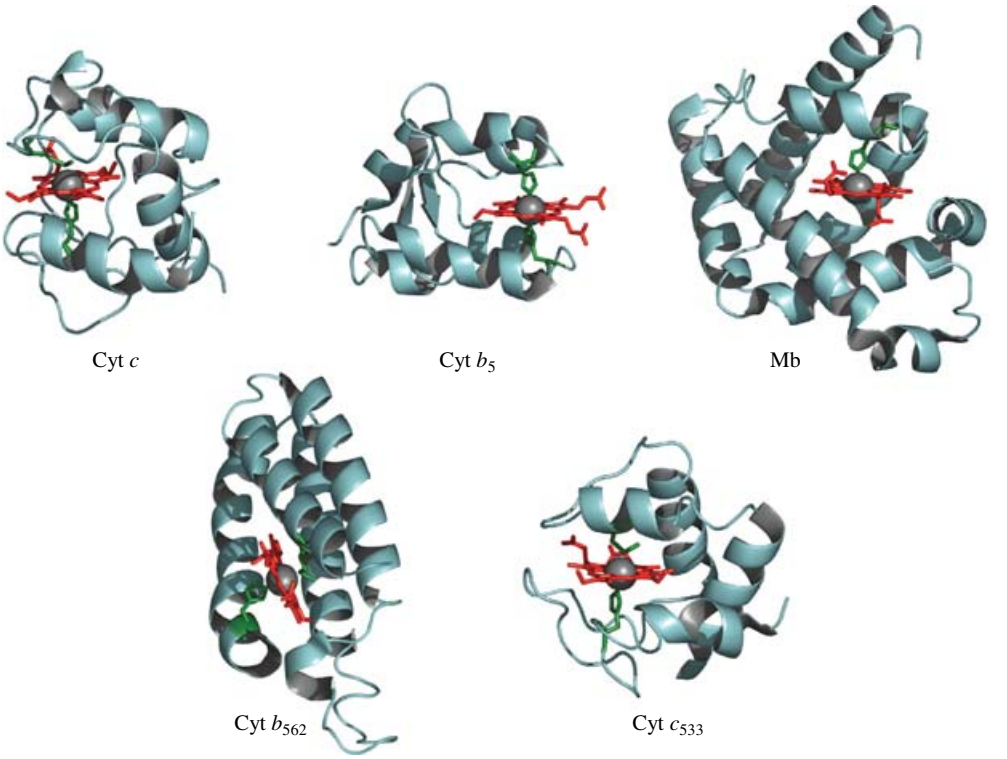

Fig. 5. Illustrations of heme-binding proteins discussed in the text. Horse heart cytochrome *c* (1AKK), *Desulfovibrio vulgaris* cytochrome c_{553} (1DVH), horse heart myoglobin (Mb) (1A6G), *E. coli* cytochrome b_{562} (1QPU), microsomal rat cytochrome b_5 (1AQA). The hemes are shown in red, with irons with grey filling; the iron-coordinating ligands are shown in green stick representations.

2002). We note that in contrast to azurin, the polypeptide does not fold in the absence of heme in the case of *c*-type cytochromes; thus, no correlating apo-protein studies are possible. Nonetheless, studies on horse and yeast cytochrome *c* proteins supporting the view that non-native heme ligation (mainly non-native histidines, but there also may be contributions from non-native methionines and the N-terminus) slows down cytochrome *c* folding at neutral pH and pathways involving misfolded intermediates have been proposed. Cytochrome *c* begins to fold on the μs time-scale but the reaction is not completed until after hundreds of ms or seconds. However, at low pH, where histidine protonation weakens coordination to the heme iron, cytochrome *c* folding on faster time-scales (folding time of 10–20 ms) is greatly enhanced (Sosnick *et al.* 1994; Pierce & Nall, 1997).

The use of contemporary laser-triggered methods, based on ligand dissociation of unfolded CO-bound reduced cytochrome *c* and electron injection into unfolded oxidized cytochrome *c*, have allowed for ns to μs time resolution (Jones *et al.* 1993; Chan *et al.* 1996; Mines *et al.* 1996). The earliest events detected by transient absorption in such studies of reduced cytochrome *c* folding at neutral pH (τ of 2 and 50 μs) were assigned to formation of His18-Fe-Met80 and His18-Fe-His26/33 (i.e. bis-His) heme ligations respectively (Jones *et al.* 1993; Chan *et al.* 1996). Subsequently, time-resolved far-UV circular dichroism (CD), directly probing the secondary structure, was coupled to electron-transfer-triggered folding of reduced horse heart cytochrome *c* (Chen *et al.* 1999). This far-UV CD study indicated that in $<$4 ms (i.e. in the dead-time of

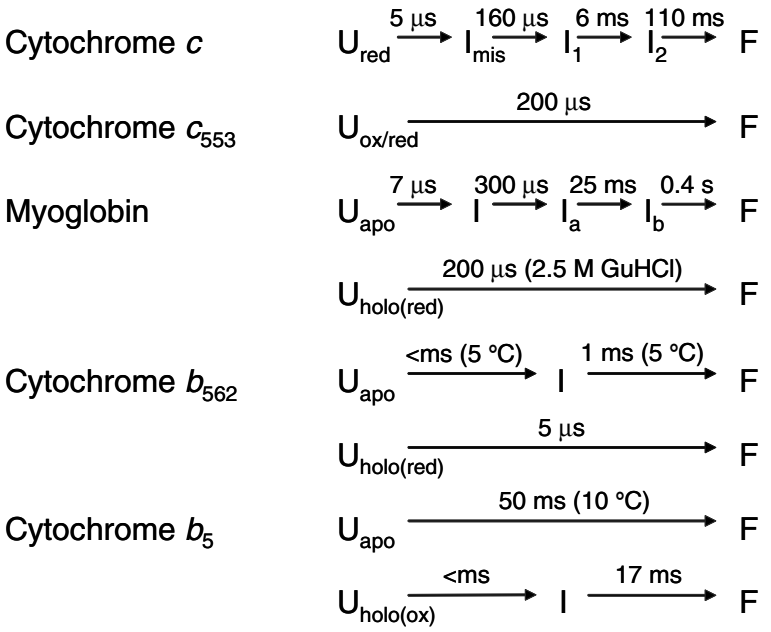

Fig. 6. Kinetic mechanisms for folding of heme-binding proteins. All time constants refer to final conditions of pH 7, 20 °C and no denaturant present, unless otherwise is stated. The data is taken from the following references: cytchrome *c* (Chen *et al.* 1999), cytochrome c_{553} (Guidry & Wittung-Stafshede, 2000a), myoglobin (Ballew *et al.* 1996; Jamin & Baldwin, 1998; Wittung-Stafshede *et al.* 1998a; Uzawa *et al.* 2004), cytochrome b_{562} (Wittung-Stafshede *et al.* 1999; Garcia *et al.* 2005), cytchrome b_5 (Manyusa *et al.* 1999; Manyusa & Whitford, 1999). U indicates unfolded, F means folded; apo- or holo-forms as well as redox states, for the *c*-type heme proteins, are indicated by subscripts.

stopped-flow experiments) there is formation of ~25% of the native structure. The kinetics of secondary structure formation was best described by four phases: initial formation (within 5 μs) of a misfolded species which has ~20% of the native structure that is followed by a small unfolding reaction between 16 μs and 1 ms and two final folding phases with time constants of 6 and 110 ms which result in the formation of the native protein (Chen *et al.* 1999). It is probable that the four phases do not represent sequential steps in a single folding pathway, but instead represent heterogeneous folding of several fractions. Later studies, comparing tuna and horse heart cytochrome *c* far-UV CD μs kinetics, suggested that the fast-folding fraction (leading to the misfolded species) of horse heart cytochrome *c* must have a His18-Fe-His33 heme configuration (Chen *et al.* 2004) (Fig. 6).

Cytochrome c_{553} from the sulfate-reducing *Desulfovibrio vulgaris* bacteria (Blackledge *et al.* 1995a) is smaller in size than the eukaryotic proteins (i.e. 79 compared to 100–120 residues), but retains the essential structural characteristics present in all class I cytochromes (Fig. 5). Comparisons of the structure of cytchrome c_{553} to structures of representative cytochromes from eukaryotic (e.g. tuna cytochrome *c*) and small bacterial (e.g. *P. aeruginosa* cytochrome c_{551}) families display striking structural similarities despite little sequence identity (Blackledge *et al.* 1995a, b, 1996). In contrast to horse heart, yeast and tuna cytochrome *c*, the heme iron (both oxidized and reduced) in unfolded cytchrome c_{553} was shown to be in a high-spin state at neutral pH (Wittung-Stafshede, 1999). Studies of the folding kinetics of cytchrome c_{553} at neutral pH may thus pinpoint the folding pathway for cytochrome *c* proteins without interference from misligated species.

We found that the kinetic traces for unfolding and refolding at pH 7 of oxidized and reduced cytochrome c_{553} were best fitted by mono-exponential decay equations, implying a two-state kinetic mechanism (Guidry & Wittung-Stafshede, 2000a). The folding time in water for oxidized cytochrome c_{553} was estimated to be <200 μs, and the reduced protein folded even faster (Fig. 6). The folding speed for oxidized cytochrome c_{553} (pH 7) is 100-fold faster than that for cytochrome *c* at low pH and at least 1000-fold faster than that for cytochrome *c* proteins at neutral pH (Guidry & Wittung-Stafshede, 2000b). Clearly, non-native iron ligations, during or prior to folding, dramatically affect the folding free-energy landscape for *c*-type heme proteins.

The tertiary structure of Mb (which has the so-called globin fold) is made up of eight α-helices, termed helix A to helix H, that surround the heme group in a hydrophobic pocket-like structure. The heme iron is non-covalently linked to His93 (Fig. 5). Like cytochrome *c*, Mb is one of the most thoroughly studied proteins with respect to folding albeit most investigations have been concerned with the apo-form (Ballew *et al.* 1996; Jamin & Baldwin, 1996, 1998). Apo-Mb adopts a structure similar to that of holo-Mb; seven of the eight α-helices are formed in apo-Mb. Apo-Mb is easily unfolded and several partially folded states can be populated at equilibrium by adjusting pH, salt concentration, and temperature. It has been demonstrated that upon lowering the pH, apo-Mb unfolds through a compact intermediate, similar to a molten globule composed of helices A, G, and H (Jamin & Baldwin, 1996, 1998). This intermediate is also formed rapidly (i.e. in the stopped-flow dead time) in the kinetic process of forming native apo-Mb at pH 6. It was demonstrated that the pH 4-stable intermediate coexists in two distinguishable forms; both appear to be on-pathway intermediates in refolding of acid- as well as urea-denatured apo-Mb (Jamin & Baldwin, 1998). Complete folding of apo-Mb occurs within 1 s at pH 6, 20 °C.

With a pioneering method, involving a rapid-mixing device combined with far-UV CD and small-angle X-ray scattering detection, researchers were able to detect sub-ms folding dynamics of apo-Mb in terms of helical content (far-UV CD) and radius of gyration (X-ray scattering) respectively (Uzawa *et al.* 2004). Folding of apo-Mb from the acid-unfolded state was initiated by a jump from pH 1·2 to pH 6. A significant collapse, corresponding to $\sim$50% of the overall change in radius of gyration from unfolded to native conformations, was observed within 300 μs after the pH jump. This intermediate displayed a globular shape and the helical content corresponded to 33% of that of the native state of apo-Mb at pH 6 (Uzawa *et al.* 2004). The early events in refolding of apo-Mb has also been followed by tryptophan-fluorescence changes upon a laser-induced temperature-jump (Ballew *et al.* 1996). This method allowed investigations in a 15 ns to 0·5 ms time window. The earliest step observed during apo-Mb folding, when jumping from the cold-denatured state at 0 °C to 22 °C, which favors folded apo-Mb, was a kinetic process completed in <20 μs. This phase was assigned to the formation of a compact, but still strongly hydrated, state of apo-Mb. Experiments on Mb mutants and consideration of steady-state CD and fluorescence spectra indicated that the observed μs phase correlated with assembly of the A·H·G helix sub-structure (Ballew *et al.* 1996). Notably, the time constant detected for the collapse into the compact apo-Mb state is similar to that expected for pure diffusion (Hagen & Eaton, 2000).

Studies targeting folding and stability of holo-Mb are not as frequent as those focused on apo-Mb. In equilibrium-unfolding studies it was shown that heme affinity is directly correlated with Mb stability (Hargrove *et al.* 1994; Hargrove & Olson, 1996). Upon unfolding of Mb bound to an oxidized heme coordinating cyanide [i.e. so called cyanomet (CN-Met) Mb], it was reported that refolding occurred by a first phase with rate constant of $\sim 1\ s^{-1}$, where structure forms around the heme, followed by a slower ligand-exchange process (suggested to be exchange of

CN to the native-histidine heme ligand), that allowed for complete polypeptide folding with half time of ~1 ms (Chiba *et al.* 1994). In this study, it was proposed that the CN-Met heme bound to the polypeptide in the stopped-flow dead-time. Only in the case of oxidized (Met) holo-Mb, has the heme been directly shown to retain interactions with the unfolded polypeptide, presumably to His93 (Wittung-Stafshede *et al.* 1998a; Moczygemba *et al.* 2000). Refolding of unfolded Met-Mb, as probed in stopped-flow experiments, was found to proceed in a simple two-state kinetic reaction with a folding time in water of ~3 s (Moczygemba *et al.* 2000). Since these experiments were free of missing amplitude, there did not appear to be sub-ms phases when the heme is present in the unfolded state. In addition, laser-induced electron-transfer-triggered folding experiments demonstrated that deoxy-Mb refolded rapidly (time constant of 200 μs at 2·5 M GuHCl; independent of protein concentration) upon reduction of unfolded, Met-Mb (Wittung-Stafshede *et al.* 1998b).

Cytchrome b_{562} from the periplasm of *E. coli* is a 106-residue cytochrome, containing a non-covalently bound heme cofactor like Mb. The heme in cytochrome b_{562} coordinates to Met7 and His102 within a four-helix bundle protein structure (Fig. 5). Like most cytochromes, the reduced form of cytochrome b_{562} is thermodynamically more stable than the oxidized form. Both chemical-denaturant and thermal-melting studies unraveled that the oxidized heme remained specifically bound to the unfolded cytochrome b_{562} polypeptide (Robinson *et al.* 1997, 1998; Wittung-Stafshede *et al.* 1999; Guidry & Wittung-Stafshede, 2000b). Binding studies by ITC revealed a dissociation constant of ~3 μM for the oxidized heme in the unfolded state (Robinson *et al.* 1997) while the heme affinity for folded apo-cytochrome is much higher, ~9 nM (Robinson *et al.* 1997). The ability of cytochrome b_{562} to retain heme upon unfolding, allowed laser-induced electron-transfer-triggered folding experiments to be executed between 2·2 and 3 M GuHCl; at these conditions, the oxidized protein is unfolded according to far-UV CD whereas the reduced form is folded (Wittung-Stafshede *et al.* 1999). Extrapolation of the time-resolved data revealed a folding speed in water of 5 μs for reduced cytochrome b_{562}, which is close to the estimated speed limit for protein folding based on diffusion. Such fast folding is in accord with theory since cytochrome b_{562} is a small and symmetrical helical protein; the folding speed also agreed well with the prediction based on relative contact order (Wittung-Stafshede *et al.* 1999).

The heme in cytochrome b_{562} can be chemically removed and the resulting apo-protein has been shown by NMR to retain much of the secondary and some of the tertiary structure of the holo-protein (Feng *et al.* 1994). The apo-protein has a substantial amount of solvent-exposed hydrophobic surface area and several highly mobile regions, which include both side-chains and peptide backbone (Feng & Sligar, 1991; Feng *et al.* 1994). The apo-form of cytochrome b_{562} is competent for reconstitution with heme to form the native holo-protein (Robinson *et al.* 1997) and likely represents a partially folded intermediate on the folding/assembly pathway. Apo-cytochrome b_{562} is substantially destabilized relative to the holo-form: the thermal midpoint is more than 10° lower, and enthalpy and heat-capacity changes are about one-half of the holo-protein values (Robinson *et al.* 1998).

Recent folding experiments with the apo-form of cytochrome b_{562}, using urea as the denaturant, revealed that it folded slower, via burst-phase intermediate, than the speed reported for the reduced holo-form: an overall τ of ~1 ms was determined at 10 °C for apo-cytochrome b_{562} (Garcia *et al.* 2005). The authors of this latter study also investigated the oxidized holo-protein by NMR at 2 M GuHCl and concluded that this state was rather compact. Based on this, they proposed that the difference in folding rates observed for apo- and holo-forms of cytochrome b_{562} can be explained by different starting structures (Garcia *et al.* 2005). We question this

conclusion since in the NMR experiments both buffer composition and GuHCl concentration differed from the original electron-transfer experiments (Wittung-Stafshede *et al.* 1999). In addition, the final structures are not identical for apo- and holo-forms, which limits reliable comparisons. To address the relevant pathway to folded holo-cytochrome b_{562}, folding experiments of the unfolded apo-protein were performed in the presence of free heme. It was discovered that the dominant path involved initial folding of the apo-protein followed by subsequent heme binding (Garcia *et al.* 2005). This suggests that heme binding to the unfolded polypeptide is slow; therefore, *in vivo* heme may not bind until after polypeptide folding. Nonetheless, we note that if heme is pre-bound to the denatured states of both Mb and cytochrome b_{562} (e.g. upon unfolding of the holo-forms *in vitro*), the folding speed is largely increased and the kinetic mechanism reduces to two-state (Fig. 6).

Cytochrome b_5 is a membrane protein (Spatz & Strittmatter, 1971). However, most studies on the structure and folding of the protein have been performed on the soluble fragment (i.e. the protein devoid of its membrane anchor). Unlike cytochrome b_{562}, the non-covalently attached heme group in cytochrome b_5 has bis-His ligation (Fig. 5). The folding behaviors of both apo- and holo-forms of a recombinant bovine cytochrome b_5 fragment, containing the first 104 residues, have been reported. Both apo- and holo-forms adopt folded structures and unfold in two-state equilibrium-unfolding processes. However, the holo-protein has significantly higher stability than the apo-form (i.e. 25 *versus* 7 kJ mol^{-1} at 25 °C) (Manyusa *et al.* 1999; Manyusa & Whitford, 1999). Holo-cytochrome b_5 unfolds in a bi-phasic reaction that was assigned to two types of heme environments in the folded state. The holo-protein refolds via a burst-phase intermediate that appears to involve structure around the heme site (Manyusa & Whitford, 1999). Apo-cytochrome b_5, on the other hand, unfolds and refolds in simple two-state kinetic reactions (Manyusa *et al.* 1999). The changes in visible-absorbance spectrum of unfolded holo-cytochrome b_5 indicate a disruption of the bis-His heme ligation, although the heme probably remains linked to the polypeptide via a single histidine or by hydrophobic interactions (Manyusa *et al.* 1999). Taken together, refolding of cytochrome b_5 follows different pathways in the presence and absence of heme (Fig. 6); in contrast to Mb and cytochrome b_{562}, the presence of the heme complicates the overall folding landscape for cytochrome b_5 and its presence does not decrease the time needed to reach the native state.

5. Fe-S cluster proteins

Fe-S cluster proteins (Fe-S proteins) are present in all living organisms and exhibit diverse functions. They contain clusters of iron and sulfur atoms with variable nuclearity and complexity. The most extensively studied proteins contain either a single cluster (e.g. [2Fe-2S], [3Fe-4S], or [4Fe-4S]), or incorporates two clusters (e.g. [4Fe-4S]/[4Fe-4S] or [3Fe-4S]/[4Fe-4S] cluster combinations) (Fig. 7). Despite several studies on the biophysical and spectroscopic properties of Fe-S proteins (Lippard & Berg, 1994), there are few folding and stability studies of these proteins. Attempts to study Fe-S protein folding have failed for many years, due to chemical destruction of the Fe-S cluster during unfolding of the polypeptide which resulted in irreversibility. Nonetheless, there are some promising technical advances and interesting observations on partially unfolded forms that deserve attention.

A partly unfolded state of the [4Fe-4S] high-potential Fe-S protein (HiPIP) isolated from *Chromatium vinosum* was characterized by NMR spectroscopy. It was demonstrated that the

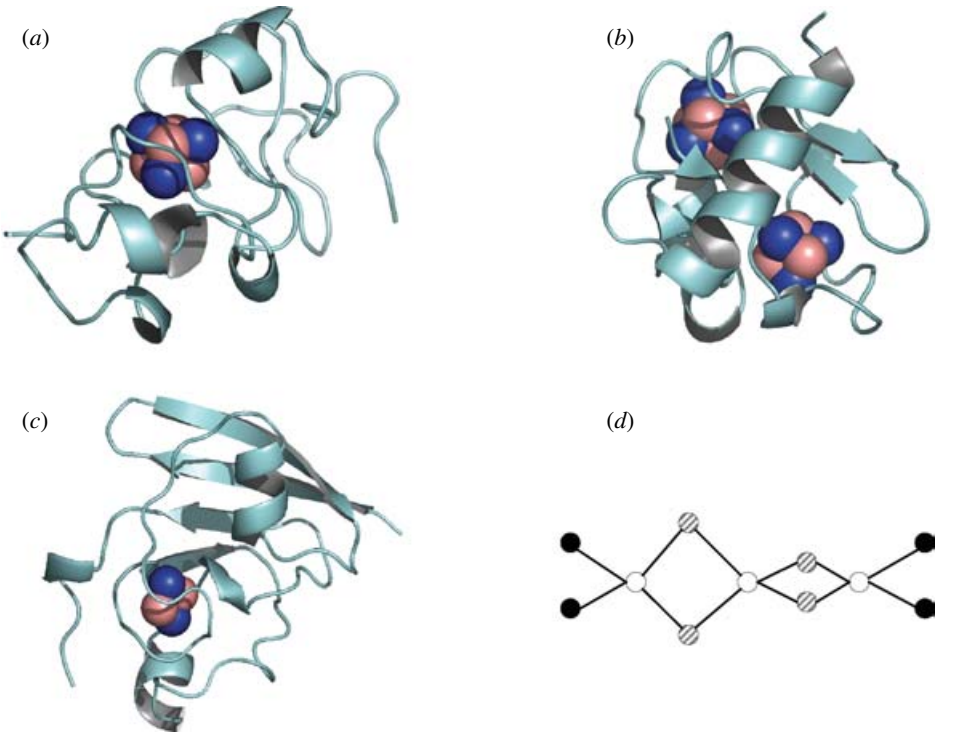

Fig. 7. Illustrations of Fe-S cluster proteins discussed in the text. (*a*) *Chromatium vinosum* HiPIP (1HRR) with [4Fe-4S] cluster. (*b*) Ferredoxin from *Bacillus schlegelii* (1BD6) with [3Fe-4S] and [4Fe-4S] clusters. (*c*) Spinach ferredoxin (1A70) with [2Fe-2S] cluster. (*d*) Scheme of linear three-iron cluster (white, iron; striped, sulfur; black, cysteine sulfurs). The cluster irons are shown in red and sulfurs in blue.

intermediate species maintains the Fe-S center, exhibits a largely collapsed secondary structure and undergoes fast cluster decomposition upon oxidation (Bertini *et al.* 1997; Bentrop *et al.* 1999). Subsequently, the generality of this behavior was addressed by similar NMR studies on [2Fe-2S] ferredoxin from *Porphyra umbilicalis*, the [3Fe-4S]/[4Fe-4S] ferredoxin from *Bacillus schlegelii*, the HiPIP from *Ectothiorhodospira halophila*, and the [4Fe-4S]/[4Fe-4S] ferredoxin from *Clostridium pasteurianum* (Bertini *et al.* 1998). It was found that the HiPIP and the [4Fe-4S]/[4Fe-4S] ferredoxin adopt intermediates that are characterized by a bound cluster in a largely unfolded polypeptide upon additions of GuHCl. However, no intermediates were observed in the case of the [3Fe-4S]/[4Fe-4S] and [2Fe-2S] ferredoxins, which were tentatively explained by a high intrinsic stability provided by structural elements other than the clusters in these proteins. Taken together, these studies led to the hypothesis that the formation of a cysteine-coordinated cluster within a still largely unfolded protein is a reasonable intermediate in the *in vivo* folding/assembly pathway of [Fe-S] proteins.

In experiments on spinach [2Fe-2S] ferredoxin using far-UV CD and visible-absorption detections, urea-treatment led to a transient state in which the polypeptide was partially unfolded but the cluster was still bound. This state subsequently converted to the completely denatured form, which lacked the cluster (Pagani *et al.* 1986). It was shown that chemical removal of the Fe-S cluster in spinach ferredoxin induced protein unfolding. In accord, characterization of the apo-protein by far-UV CD revealed a disordered structure in solution (Pagani *et al.* 1986).

Enzymatic reconstitution of the holo-form of spinach ferredoxin resulted in the return of the native structure. It appears, at least in the case of spinach ferredoxin, that cluster insertion is a prerequisite for the polypeptide to fold properly.

A novel *linear* [3Fe-4S] cluster (Fig. 7) was observed for the first time in 1984 when beef heart aconitase, which is a [4Fe-4S] protein, was incubated at pH values higher than 9·5 or treated with 4–8 M urea (i.e. the so-called purple aconitase) (Kennedy *et al.* 1984). That this partially unfolded form of the protein indeed contained a linear [3Fe-4S] cluster was concluded from the characteristic absorption peaks at 520 and 610 nm, EPR and Mössbauer data and comparison to model complexes (Hagen *et al.* 1983). Purple aconitase was stable for days at 4 °C in the presence of air but subsequently decomposed (Kennedy *et al.* 1984). To date, linear [3Fe-4S] clusters have been detected *in vitro* in many different proteins. In most cases, the clusters are triggered to form from either cubic [3Fe-4S] or [4Fe-4S] clusters upon polypeptide-structural perturbations. To our knowledge, linear [3Fe-4S] clusters have been observed transiently in the following proteins: *Thermus thermophilus* [3Fe-4S]/[4Fe-4S] ferredoxin, *Sulfolobus acidocaldarius* [3Fe-4S]/[4Fe-4S] ferredoxin, *Acidianus ambivalens* [3Fe-4S]/[4Fe-4S] ferredoxin, bovine heart [4Fe-4S] aconitase, *E. coli* [4Fe-4S] dihydroxy acid dehydratase, *Rhodothermus marinus* [3Fe-4S] ferredoxin, and human [3Fe-4S] iron regulatory protein 1 (IRP) (Gailer *et al.* 2001; Moczygemba *et al.* 2001; Jones *et al.* 2002; Griffin *et al.* 2003). In all cases, except the last that appeared at physiological conditions (Gailer *et al.* 2001), high pH and the presence of denaturant was required for linear [3Fe-4S] cluster formation. For the *A. ambivalens* and *S. acidocaldarius* ferredoxins, the rate of linear [3Fe-4S] cluster formation correlated with the protein-unfolding speed (secondary structure disappearance), whereas the subsequent linear cluster degradation rate was independent of denaturant concentration but depended on pH (Jones *et al.* 2002). However, a recent report questions the observation of linear clusters in *A. ambivalens* ferredoxin (Leal *et al.* 2004).

Surprisingly, linear [3Fe-4S] clusters also form upon GuHCl-induced unfolding of *Aquifex aeolicus* [2Fe-2S] ferredoxins, namely *Aae*Fd1, *Aae*Fd4 and *Aae*Fd5, at alkaline conditions (pH 10, 20 °C). In contrast to seven-, four-, and three-iron ferredoxins, [2Fe-2S] proteins need to acquire additional iron and sulfur to form the linear clusters. We found the mechanism of linear [3Fe-4S] cluster formation in the [2Fe-2S] proteins to depend critically on the speed of polypeptide unfolding (Higgins & Wittung-Stafshede, 2004). In similarity to seven-iron proteins, polypeptide unfolding determined the rate by which linear [3Fe-4S] clusters form in *Aae*Fd4 and *Aae*Fd5. In contrast, in a disulfide-lacking variant of *Aae*Fd1, which unfolds faster than *Aae*Fd4 and *Aae*Fd5, the polypeptides unfold first and the majority of clusters decompose. Next, unfolded polypeptides retaining intact clusters scavenge iron and sulfur to form linear [3Fe-4S] clusters in a bimolecular reaction that is similar to inter-protein cluster transfer rates. Wild-type *Aae*Fd1, which has an intact disulfide, unfolds slower than the speed of linear cluster decomposition and the linear species is never populated (Higgins & Wittung-Stafshede, 2004). Albeit linear [3Fe-4S] clusters have no known biological role, they may be intermediates during folding of Fe-S proteins.

There is only one study in which the thermodynamic stability of the apo- and holo-forms of a Fe-S protein has been directly compared. Experimental conditions including sodium sulfide and mercaptoethanol allowed, for the first time, reversible thermal unfolding of a Fe-S protein (Burova *et al.* 1995). The protein used was adrenal ferredoxin (i.e. adrenodoxin), which is a 128- residue protein with a [2Fe-2S] cluster. At these conditions, equilibrium unfolding of the holo-protein was a two-state process and the cluster remained bound to the unfolded polypeptide. This observation further emphasizes the question of whether the holo- or the apo-form of

Fe-S proteins is the relevant species *in vivo* during intracellular transport and folding (Burova *et al.* 1995). When the cluster is removed from adrenodoxin, the transition temperature (T_m) and the unfolding enthalpy change is considerably reduced; the holo-form has a T_m of 51 °C in the presence of 10 mM Na_2S; the apo-form has a T_m of 37 °C. In addition, the apo-protein is much more susceptible to protease digestion than the holo-protein (Burova *et al.* 1995). More recently, conditions including DTT have been reported by the same group to allow for both reversible chemical and thermal unfolding of adrenodoxin (Bera *et al.* 1999). It was proposed that DTT prevents damage of the Fe-S cluster during protein unfolding by partial coordination to the cluster. This may be of biological relevance since analogous cluster stabilization could occur *in vivo*, where strong reducing agents, such as glutathione, are present. Moreover, this work (Bera *et al.* 1999) should make *in vitro* biophysical studies of the kinetic mechanisms of Fe-S protein folding/assembly possible; currently nothing is known.

6. Metallopeptides

The so-called zinc finger (ZF) is one of the most prevalent metal-binding motifs found in proteins (Berg & Shi, 1996; Wolfe *et al.* 2000). Most ZFs serve as DNA-binding domains in proteins that regulate gene expression. However, recent work has demonstrated that ZFs can also mediate protein–protein and protein–lipid interactions (Matthews & Sunde, 2002). Sequence-specific DNA recognition is achieved by the concerted interaction of several ZFs connected by short peptide linkers within the same polypeptide. Solution structures of tandem ZFs bound to DNA show a characteristic wrapping of the ZF around the DNA, making base-specific contacts in the major groove (Dyson & Wright, 2004). Although tandem ZF motifs are covalently linked, the individual units are independently folded and behave largely as beads on a string in the absence of DNA.

There are at least 14 different classes of ZFs, which differ in their exact amino-acid sequences and spacing of the zinc-binding residues (Matthews & Sunde, 2002). The *classic* ZF motif is a peptide comprised of ~30 residues that is folded around a Zn^{2+}: the consensus sequence is **Φ**-X-**C**-X_{2-5}-**C**-X_3-**Φ**-X_5-**Φ**-X_2-**H**-X_{2-5}-**H**. Here X represents any amino acid, **Φ** a hydrophobic residue and the bold letters [two cysteines (C) and two histidines (H)] represent the side-chains that coordinate Zn^{2+} (Klug & Schwabe, 1995), most often in a tetrahedral geometry (Maret & Vallee, 1993). The zinc binds tightly; the dissociation constant for a typical ZF-Zn^{2+} complex is ~10 pM. The zinc may be exchanged for other divalent metal ions *in vitro* although this reduces the affinity (e.g. the affinity for Co^{2+} to a typical ZF peptide is only in the mM–μM range) (Lachenmann *et al.* 2004). NMR and CD experiments have demonstrated that modifications or eliminations of the zinc ligands, or the conserved hydrophobic residues, in ZF peptides strongly affect the metal affinity (Parraga *et al.* 1990).

The ZF motif is comprised of a short anti-parallel β-sheet in the N-terminal region and an α-helix in the C-terminal region (i.e. the so-called $\beta\beta\alpha$ fold), which are arranged in a hairpin structure. This structure is stabilized by zinc coordination and by hydrophobic interactions between the conserved hydrophobic residues. Without the metal, the ZF peptide adopts an extended β-sheet structure in the N-terminal region while the α-helix region is unstructured and there is no tertiary structure (Miura *et al.* 1998). In earlier work (Frankel *et al.* 1987), it was shown that metal coordination by a ZF peptide occurred in parallel with secondary and tertiary structure formation, this result was later confirmed by NMR (Frankel *et al.* 1987; Parraga *et al.* 1990). Using

Raman spectroscopy it was found that the cysteine residues bind to the Zn^{2+} prior to co-ordination of the histidines. However, coordination to all four ligands was necessary to induce the transition from the extended β-sheet to the native $\beta\beta\alpha$ fold (Miura *et al.* 1998). Clearly, zinc coordination is essential for folding of ZF domains in proteins; however, there are no detailed kinetic studies of the folding/binding free-energy landscape.

The amyloid β (Aβ) peptide is the major constituent of senile plaques in the brains of patients with Alzheimer's disease (AD) (Masters *et al.* 1985; Selkoe *et al.* 1986; Miura *et al.* 2000). The peptide is generated by the proteolytic cleavage of the amyloid precursor protein. Upon cleavage Aβ is released into extracellular fluids as a soluble peptide. The most predominant peptides, Aβ (residues 1–40) and Aβ (residues 1–42), are found in the cerebrospinal fluid and/or blood plasma of all humans. The N-terminal portion of the Aβ peptide is hydrophilic, whereas the C-terminus (i.e. residues 29–42) is rich in hydrophobic residues (Syme *et al.* 2004). Under physiological conditions yet to be determined, Aβ is converted from its soluble form to amyloid fibrils. Deposition in the brain of such insoluble aggregates of Aβ causes neuro-degeneration. Several studies have demonstrated that Cu^{2+} and Zn^{2+} promote aggregation of Aβ *in vitro*. *In vivo* high concentrations of Cu^{2+} (0·4 mM) and Zn^{2+} (1 mM) have been reported in aggregates isolated from diseased brains (Lovell *et al.* 1998; Raman *et al.* 2005). It has been shown *in vitro* that, Zn^{2+} ions induce Aβ aggregation at pH >6, whereas Cu^{2+} is only effective between pH 6 and 7. Raman spectroscopy and NMR have demonstrated that three histidines situated in the N-terminal hydrophilic region constitute the primary metal-binding sites. Upon Zn^{2+} binding to one histidine, peptides aggregate through intermolecular His-Zn^{2+}-His bridges. The same mechanism is proposed for Cu^{2+}-induced Aβ aggregation (Miura *et al.* 2000; Petkova *et al.* 2002). X-ray diffraction, Fourier-transformed infrared spectroscopy (FTIR), NMR, and far-UV CD show a conversion from random coil to an extended β-sheet-like conformation upon metal-Aβ complexion and peptide aggregation (Lansbury *et al.* 1995; Inouye & Kirschner, 1996; Tjernberg *et al.* 1999; Syme *et al.* 2004). This strongly suggests that metals catalyze the formation of fibrils, although their mechanistic roles are not clear.

De novo designed metallopeptides and metalloproteins provide an excellent opportunity to study the interplay between metal binding and protein folding under restricted conditions. The most exploited motif in *de novo* design is the α-helical coiled-coil structure. This motif typically consists of two, three, or four amphipathic α-helices and each helix is composed of several heptad repeats. The seven residues that constitute each repeat are typically denoted by the letters *abcdefg* (Ghosh & Pecoraro, 2004). The oligomeric state of coiled-coils can be controlled by amino-acid selection and by the incorporation of specific metal ligands, most often cysteines, histidines and glutamic-acid residues (DeGrado *et al.* 1999; Ghosh & Pecoraro, 2004). Among the first *de novo* metallopeptides to be studied were two 15-residue peptides. One peptide incorporated two histidines and the other contained one cysteine and one histidine: together, these four residues formed the ligand set necessary for divalent metal-ion coordination. Peptide binding to Cd^{2+}, Cu^{2+}, Ni^{2+}, and Zn^{2+} were demonstrated by CD experiments and in every case, an enhancement in peptide α-helix content was observed upon metal binding and dimerization (Ghadiri & Choi, 1990). It has been shown in other systems that mostly unstructured peptides fold into α-helices and assemble upon metal coordination (Kohn *et al.* 1998a, b; Suzuki *et al.* 1998; Kiyokawa *et al.* 2004).

In another family of *de novo* metallopeptides (based on the so-called TRI peptide), the four repeats of the heptad Leu_a-Lys_b-Ala_c-Leu_d-Glu_e-Glu_f-Lys_g was used as the starting point (O'Neil & DeGrado, 1990; Betz *et al.* 1995; Bryson *et al.* 1995; Dieckmann *et al.* 1998). In each peptide a

single cysteine residue at either the *a* or *d* position was introduced producing a thiol-rich environment that allowed for Hg^{2+} binding. In the apo-form, these peptides exist in equilibrium between monomers, dimers and trimers. The favored order of assembly, i.e. two- or three-stranded α-helical coiled-coils, is highly pH-dependent. Metal-binding affected the equilibrium between dimers and trimers, although there was no increase in secondary structure upon Hg^{2+} binding. Thus, in contrast to the shorter peptides discussed above, this family of peptides appear to be rigid building blocks. Nonetheless, metal coordination substantially increased the overall stability of the α-helices toward perturbation by GuHCl (Dieckmann *et al.* 1998).

The kinetics of metal-induced peptide folding was investigated in detail for a three-stranded coiled-coil system that was unfolded without metals; here, peptides included only three heptad repeats from the TRI peptide. In combination with far-UV CD experiments, stopped-flow mixing was used to monitor metal coordination (Farrer & Pecoraro, 2003). The deduced mechanism for this metal-peptide system involves a rapid (i.e. <4 ms) initial collapse of two peptides due to cysteine coordination of Hg^{2+}, forming a transient Hg-$(peptide)_2$ complex with a linear S(Cys)-Hg-S(Cys) metal geometry. This rapid step is followed by a slower incorporation of the third peptide, forming the three-stranded coiled-coil. This step involved two different pathways; one that has the third helix properly folded and quickly undergoes cysteine thiol de-protonation that yields the desired three-stranded coiled-coil with a trigonally-coordinated Hg^{2+}. The other path involves a species that is misfolded and has to rearrange in an even slower step before the properly folded structure is reached. The overall reaction time to adopt the three-stranded coiled-coil in the presence of metal ions is $\sim$10 s (pH 8·5, 10 $^{\circ}$C) (Farrer & Pecoraro, 2003; Ghosh & Pecoraro, 2004).

7. Other metalloproteins

In addition to the already discussed groups of proteins, there are limited folding/stability data on a range of other metalloproteins that we will briefly mention here. That metals stabilize the folded forms of metalloproteins appear to be general phenomena that are valid regardless of whether the metal remains bound after polypeptide unfolding or not. For example, the Mg^{2+} ion in CheY, the Cu^{2+} and Zn^{2+} ions in SOD, and the Ca^{2+} ions in calmodulin (CaM) clearly stabilize the folded structures (Mei *et al.* 1992; Filimonov *et al.* 1993).

CheY is a signal-transduction protein that regulates bacterial chemotaxis via reversible phosphorylation of Asp57. The Mg^{2+} is coordinated by Asp13, Asp57, the carbonyl backbone of Asn59, and three water molecules in a peptide loop near the protein surface (Sola *et al.* 2000). CheY has a structure that belongs to the flavodoxin-like fold. This fold (a five-stranded parallel β-sheet surrounded by α-helices at either side) is one of the five most common folds and is shared by 16 protein superfamilies according to the SCOP database (including, for example, catalases, chemotactic proteins, lipases, esterases and flavodoxins). These families, despite the same overall structure, comprise a broad range of unrelated proteins with different functions and thus different cofactors and/or active sites (Muller, 1992). This variety implies that a cofactor bound to this structural motif may not have any significant effect on protein stability. Nonetheless, equilibrium-unfolding experiments have demonstrated that the presence of high concentrations of Mg^{2+} greatly enhance (up to 30%) the stability of CheY (Filimonov *et al.* 1993). In similarity, although the cofactor is not a metal, the flavin mononucleotide (FMN) cofactor in flavodoxin (which binds to the same loop region as the Mg^{2+} in CheY) stabilizes the

native form by 25% (Apiyo & Wittung-Stafshede, 2002). In this latter system, kinetic experiments revealed that the presence of bound FMN in the unfolded state simplified the kinetic-folding mechanism to two-state and speeded-up the reaction (Apiyo & Wittung-Stafshede, 2002).

In SOD, Cu^{2+} plays a catalytic role and Zn^{2+} has a structural role (Tainer *et al.* 1983; Battistoni *et al.* 1998; Banci *et al.* 2003). SOD is a large dimer held together by hydrophobic interactions and an inter-protein disulfide bridge. Although equilibrium-unfolding of SOD is not two-state, it is clear that the holo-form is substantially more stable than the apo-form towards chemical perturbation: unfolding is completed at 6 M and 3 M GuHCl for holo- and apo-forms respectively (Mei *et al.* 1992).

CaM is a 148-residue protein which is involved in a variety of physiological processes. The protein has two homologous domains, each containing a pair of EF hands (helix-loop-helix motifs); each EF hand is capable of binding a Ca^{2+} ion which results in a total of four metals per protein. Each Ca^{2+} is coordinated by seven ligands: three aspartates or asparagines, one glutamate, one backbone carbonyl, and one water molecule (Lippard & Berg, 1994). NMR and far-UV CD studies have shown that the apo-form of CaM has a partially unfolded C-terminal domain but an N-terminal domain almost fully folded (Finn *et al.* 1995; Kuboniwa *et al.* 1995; Masino *et al.* 2000). Upon Ca^{2+} binding both domains become completely structured. Urea-induced equilibrium unfolding of CaM is three-state regardless of the presence or absence of Ca^{2+} (20 °C, pH 8) (Masino *et al.* 2000). Interestingly, the C-terminal domain unfolds prior to the N-terminal domain in the case of the apo-form [$\Delta G_U(H_2O) = 3{\cdot}55$ kcal mol^{-1} for N-terminal domain and 1·45 kcal/mol for C-terminal domain] whereas, for the holo-form, the order is reversed [$\Delta G_U(H_2O) = 4{\cdot}72$ kcal/mol for N-terminal domain and 6·45 kcal mol^{-1} for C-terminal domain] (Masino *et al.* 2000). Taken together, the holo-form of each domain of CaM is significantly more stable than the apo-form; the largest effect occurs for the C-terminal domain.

For a few proteins, the kinetic origin of the stabilizing effect by the metal has been addressed. In the case of both *E. coli* ribonuclease H1 (RNase H1), which binds Mg^{2+}, and staphylococcal nuclease A (SNase A), which binds Ca^{2+}, the kinetic-folding reactions are best described by three-state mechanisms that are not affected by the presence or absence of metals (Sugawara *et al.* 1991; Goedken *et al.* 2000). In both cases, the metals appear to stabilize the proteins *via* slower unfolding kinetics. Furthermore, in the case of RNase H1, it was shown that Mg^{2+} dissociates upon unfolding and only rebinds to the fully folded state (Goedken *et al.* 2000).

In contrast to RNase H1 and SNase A, the stabilizing effects of the metals in carbonic anhydrase (Zn^{2+}) and α-lactalbumin (Ca^{2+}) appear to be due to increased protein-folding speeds (Yazgan & Henkens, 1972; Wong & Hamlin, 1975; Forge *et al.* 1999). Equilibrium studies have demonstrated that GuHCl-induced unfolding of apo and Zn^{2+} forms of carbonic anhydrase is a three-state process that proceeds through molten-globule intermediates (Henkens *et al.* 1982). The Zn^{2+} ion stabilizes both the native and the molten-globule states (Andersson *et al.* 2001). Thus, the cofactor must remain bound to the intermediate form. Folding kinetics for both apo and Zn^{2+} forms of carbonic anhydrase are multi-phasic: still, the overall refolding time is shorter in the presence of Zn^{2+} implying that the metal remains bound also to the unfolded state, or that it rebinds early in the kinetic-refolding process (Yazgan & Henkens, 1972; Wong & Hamlin, 1975). For α-lactalbumin (α-LA), the region that constitutes the Ca^{2+}-binding site becomes structured early in the kinetic-refolding reaction and the overall refolding speed is more than two orders of magnitude faster in the presence of Ca^{2+} (Kuwajima *et al.* 1989; Forge *et al.* 1999).

This acceleration of folding is consistent with the Ca^{2+} ion binding to partially folded species formed early in the refolding reaction (Forge *et al.* 1999).

8. Metalloprotein assembly *in vivo*

In vivo, translation of gene messages into functional proteins should be rapid for efficient maintenance of cellular activities. We have demonstrated that although polypeptide-folding speed is not increased, *active* azurin forms many orders of magnitude faster when the copper is allowed to interact with the unfolded polypeptide, instead of with the folded protein (Fig. 4). Together with similar *in vitro* data on several other proteins (e.g. heme proteins, flavodoxin, carbonic anhydrase, α-LA), this implies that binding of metals prior to polypeptide folding may be one method to assure adequate formation of active metalloproteins *in vivo*.

We note that in the case of copper, such ions are almost non-existent in their free form in the cytoplasm (O'Halloran & Culotta, 2000) since copper's redox properties may result in oxidative damage of proteins, lipids, and nucleic acids. Instead, the cellular copper concentration is strictly controlled and most copper ions are delivered to their destinations by copper chaperones (Lamb *et al.* 1999, 2001). Three organelle-specific trafficking pathways for copper have been described in eukaryotes: Cox17 for mitochondrial delivery, CCS for cytosolic delivery to SOD, and ATX1 for delivery to proteins in the secretory pathway (O'Halloran & Culotta, 2000). Copper insertion in SOD is well characterized. CCS is a dimeric copper chaperone that seems specific for SOD. Interestingly, the crystal structure of yeast CCS reveals two SOD-like domains that form a homodimer. This provides a structural explanation of target recognition (Lamb *et al.* 1999). The metal-transfer step is proposed to occur upon formation of a heterodimer between one CCS and one SOD monomer. Formation of this complex, which results in conformational changes in both proteins, appears to be facilitated by the presence of zinc (Lamb *et al.* 2001).

Prokaryotes, like *P. aeruginosa*, lack intracellular compartments; thus, organelle-specific carriers of metals may not be essential. However, a homolog of ATX1 (i.e. CopZ) has been described for enteric bacteria (e.g. *Enterococcus hirae*) (O'Halloran & Culotta, 2000). *E. hirae*, which is the best understood prokaryotic copper homeostasis system, regulates copper uptake, availability, and export through a *cop* operon (Solioz & Stoyanov, 2003). The *cop* operon is composed of four structural genes which encode for a copper-responsive repressor CopY, a copper chaperone CopZ, and two copper ATPases, CopA and CopB (Solioz & Stoyanov, 2003). It is quite feasible that *P. aeruginosa* may utilize a similar copper regulator system.

Currently, little is known about copper incorporation in azurin in *P. aeruginosa* although it is believed that the polypeptide is transported to the periplasm before copper insertion (Nar *et al.* 1992a). The periplasm is not as reducing as the cytoplasm, posing the question as to which of Cu^{1+} or Cu^{2+} is inserted into azurin in *P. aeruginosa*. Since the zinc form of azurin is not a by-product *in vivo* (Nar *et al.* 1992a), either the level of copper is higher than that of zinc in *P. aeruginosa*'s periplasm or a copper chaperone is involved. We propose that if a copper chaperone is involved *in vivo*, such chaperone-mediated copper delivery is easier if azurin is unfolded with its copper ligands exposed. In folded azurin, the copper site is buried 7 Å below the surface and is shielded from solvent and other proteins (Nar *et al.* 1991). The *in vitro* observations of tight and specific copper binding to unfolded azurin support this idea.

Living systems have evolved sophisticated protein systems for solubilization, sequestion, transport, and release of iron. Transferrins transport iron into cells and release it within the endosome; the protein hemopexin delivers heme to the same compartment. The latter protein,

which is a serum glycoprotein, serves both to protect against heme toxicity and to conserve and recycle heme, especially during turnover of hemoglobin (Baker *et al.* 2003).

In the case of *c*-type cytochromes, it has been proposed that heme attachment is a required step before correct folding occurs *in vivo* (Bertini *et al.* 1994; Lippard & Berg, 1994). In most prokaryotic organisms, the cytchrome *c* gene is translated with a leader signal sequence, which is not cleaved until after translocation across the cytoplasmic membrane into the periplasm and enzymatic heme ligation by a cytochrome *c* heme-lyase enzyme has occurred (Ramseier *et al.* 1991). The heme is covalently attached by this enzyme to the two cysteines in the cytochrome via thioether linkages to the heme vinyl groups. It is believed that ligation is completed when the polypeptide is still associated with the membrane and still contains the signal sequence. After heme insertion, the signal sequence is cleaved off and the holo-protein is free to fold into its native configuration. The *in vitro* results presented here show that the subsequent folding process of the heme-linked polypeptide is strongly modulated by the presence or absence of heme ligands in the unfolded state.

While specific heme transporters and ligation enzymes appear necessary for *c*-type cytochrome assembly, a different, perhaps non-specific or diffusional, mechanism for heme transport and insertion into perplasmic cytochrome b_{562}, cytochrome b_5 and hemoglobin has been proposed based on *E. coli* studies (Goldman *et al.* 1996). Cytochrome b_{562} is translated with a leader peptide that directs the protein to the *E. coli* periplasm. Regardless of over-expression with or without the leader peptide, the majority of cytochrome b_{562} was found to accumulate as apo-protein in the cells (Goldman *et al.* 1996). This parallels the *in vitro* data and suggests that heme binding is a final step in the *in vivo* formation of active cytochrome b_{562}. This may be the pertinent path *in vivo* for the assembly of most proteins with non-covalent heme cofactors.

The development of extracellular proteins for use as oxygen-delivering pharmaceuticals has generated significant interest in the understanding of how heme binding and globin folding are coupled in Mb and hemoglobin (Hargrove *et al.* 1994; Hargrove & Olson, 1996). The thermodynamic stability of potential blood-substitute products is determined by the resistance of the holo-proteins to heme loss and subsequent protein unfolding. On the other hand, the expression yields in bacteria appear to be determined primarily by the rate and extent of apo-protein folding (Hargrove *et al.* 1994; Hargrove & Olson, 1996). This observation implies that heme insertion into Mb and hemoglobin *in vivo* requires pre-folding of the apo-protein. Further advances in this area, increasing both apo-protein stability and heme affinity, will be of great clinical importance for maximizing the safety, effectiveness, and retention time of extracellular hemoglobin-based blood substitutes.

The synthesis of Fe-S clusters *in vivo* is believed to require a complex machinery encoded in prokaryotes by the *isc* (Fe-S cluster) operon (Agar *et al.* 2000; Ollagnier-De Choudens *et al.* 2000, 2001). In addition to several open reading frames of unknown function, this operon contains genes for molecular chaperones (*hscA* and *hscB*), an electron transfer [2Fe-2S] ferredoxin (*fdx*), and three *isc* genes, *iscS*, *iscU* and *iscA*. IscS and IscU exhibit strong homology to proteins NifS and NifU, which are responsible for nitogenase Fe-S cluster biosynthesis in *Azotobacter vinelandii* (Dean *et al.* 1993; Zheng *et al.* 1993). In eukaryotes, mitochondrial proteins, highly homologous to the bacterial Isc proteins, have been shown to be involved in Fe-S cluster assembly. It has been proposed that IscU and IscA provide scaffolds for assembly of intermediate Fe-S clusters that can be subsequently used for maturation of apo-forms of Fe-S proteins (Ollagnier-De Choudens *et al.* 2001). More experiments are needed to understand cluster transfer at the molecular level. In particular, does the transfer concern the intact [2Fe-2S] or does it involve

degradation and reassembly of the cluster into the apo-protein target? It was shown for one [2Fe-2S] ferredoxin that enzymatic cluster assembly and insertion drive the polypeptide to fold *in vitro*. Taken together with the *in vitro* observations of intermediates with intact clusters but unfolded polypeptides suggest that *in vivo* Isc protein-mediated cluster insertion may precede polypeptide folding during Fe-S protein assembly.

The inter-conversion of Fe-S proteins between apo- and holo-forms, and the inter-conversion of Fe-S clusters of high and low nuclearity (i.e. between [4Fe-4S] and [2Fe-2S] forms), are mechanisms for organisms to deal with oxidative stress and changes in intracellular iron concentrations. Fe-S proteins that are dependent on cluster disassembly and conversion include novel transcriptional and translational regulators. In addition, a number of [4Fe-4S] proteins undergo reversible degradation to [2Fe-2S] forms in the presence of O_2, possibly as a protective mechanism (Bertini *et al.* 1994; Lippard & Berg, 1994). While no biological function for linear [3Fe-4S] Fe-S clusters is known, the plentiful *in vitro* observations of these suggest that they may be intermediates after unfolding, or prior to folding, of Fe-S proteins *in vivo*. It appears reasonable to postulate that protein-mediated structural perturbations can be used *in vivo* to regulate Fe-S cluster rearrangements; such events may be used to modulate or control various biological functions.

Although there are no known zinc chaperones, membrane transport and regulatory proteins specific for zinc have been identified in some organisms. The ZIP (Zrt-, Irt-like Protein) proteins control zinc transport in and out of the cytoplasm in yeast and plants (Bartsevich & Pakrasi, 1995). In *E. coli*, the *ZnuABC* gene products (including a periplasmic zinc-binding component, a membrane component and an ATPase subunit) are proposed to act as a periplasmic zinc-transport system (Patzer & Hantke, 1998). The concentration of zinc in the *E. coli* cytoplasm is regulated by two other proteins, Zur (Zinc uptake regulator) for import and ZntR (Zinc transcriptional Regulator) for export (Hitomi *et al.* 2001; Outten & O'Halloran, 2001). Whereas Zur switches off expression of the periplasmic zinc-transport machinery, ZntR up-regulates transcription of the protein ZntA, which is a zinc-export protein with a similar structure as the N-terminal domain of the copper chaperone ATX1 (Banci *et al.* 2002).

9. Concluding remarks

Despite the critical role of metalloproteins in fundamental processes *in vivo*, little is known about the biological mechanisms of metalloprotein folding and assembly (Bartnikas & Gitlin, 2001). Here we have reviewed existing *in vitro* biophysical work on the interplay between metal–protein interactions and polypeptide folding in several key protein and peptide systems. The following insights emerge:

(1) The presence of a metal often stabilizes the native protein.
(2) Metals have the ability to interact specifically with unfolded polypeptides.
(3) The presence of the cofactor is sometimes essential for the polypeptide to fold.
(4) Coordination of a metal prior to polypeptide folding can dramatically accelerate formation of functional metalloproteins.
(5) On the other hand, some polypeptides must form well-defined metal sites before metal binding can occur.

Clearly, a future challenge for investigators is to relate the processes observed *in vitro* with folding *in vivo*. For metalloproteins, this includes understanding how metal sites are assembled

within the cell and the possible role of intracellular metal-delivery proteins. We want to emphasize that conformational changes of metallopeptides play an important role in a range of human diseases. For example, Cu^{2+} and Zn^{2+} ions have been shown to induce aggregation of amyloid-forming peptides (Villanueva *et al.* 2004). Further understanding of metallopeptide and metalloprotein folding may also aid in curing of diseases related to metal metabolism, such as Menkes syndrome and Wilson's disease, which both involve erroneous cofactor–protein interactions. Clearly, the topic of metalloprotein folding offers many future challenges as well as opportunities for researchers. We hope that this review has conveyed the current status as well as the significance of this developing interdisciplinary field.

10. Acknowledgments

Financial support is provided by grants from NIH (GM059663) and the Robert A. Welch Foundation (C-1588). C.J.W. is supported by the Houston Area Molecular Biophysics Program (GM08280). We thank past and present group members for their contributions.

11. References

Adman, E. T. (1991). Copper protein structures. *Advances in Protein Chemistry* **42**, 145–197.

Agar, J. N., Krebs, C., Frazzon, J., Huynh, B. H., Dean, D. R. & Johnson, M. K. (2000). IscU as a scaffold for iron-sulfur cluster biosynthesis: sequential assembly of [2Fe-2S] and [4Fe-4S] clusters in IscU. *Biochemistry* **39**, 7856–7862.

Andersson, D., Hammarstrom, P. & Carlsson, U. (2001). Cofactor-induced refolding: refolding of molten globule carbonic anhydrase induced by Zn(II) and Co(II). *Biochemistry* **40**, 2653–2661.

Apiyo, D. & Wittung-Stafshede, P. (2002). Presence of the cofactor speeds up folding of *Desulfovibrio desulfuricans* flavodoxin. *Protein Science* **11**, 1129–1135.

Bai, Y. (1999). Kinetic evidence for an on-pathway intermediate in the folding of cytochrome c. *Proceedings of the National Academy of Sciences USA* **96**, 477–480.

Baker, H. M., Anderson, B. F. & Baker, E. N. (2003). Dealing with iron: common structural principles in proteins that transport iron and heme. *Proceedings of the National Academy of Sciences USA* **100**, 3579–3583.

Ballew, R. M., Sabelko, J. & Gruebele, M. (1996). Direct observation of fast protein folding: the initial collapse of apomyoglobin. *Proceedings of the National Academy of Sciences USA* **93**, 5759–5764.

Banci, L., Bertini, I., Ciofi-Baffoni, S., Finney, L. A., Outten, C. E. & O'Halloran, T. V. (2002). A new zinc-protein coordination site in intracellular metal trafficking: solution structure of the Apo and Zn(II) forms of ZntA(46–118). *Journal of Molecular Biology* **323**, 883–897.

Banci, L., Bertini, I., Cramaro, F., Del Conte, R. & Viezzoli, M. S. (2003). Solution structure of Apo Cu,Zn superoxide dismutase: role of metal ions in protein folding. *Biochemistry* **42**, 9543–9553.

Bartnikas, T. B. & Gitlin, J. D. (2001). How to make a metalloprotein. *Nature Structural Biology* **8**, 733–734.

Bartsevich, V. V. & Pakrasi, H. B. (1995). Molecular identification of an ABC transporter complex for manganese: analysis of a cyanobacterial mutant strain impaired in the photosynthetic oxygen evolution process. *EMBO Journal* **14**, 1845–1853.

Battistoni, A., Folcarelli, S., Cervoni, L., Polizio, F., Desideri, A., Giartosio, A. & Rotilio, G. (1998). Role of the dimeric structure in Cu,Zn superoxide dismutase. pH-dependent, reversible denaturation of the monomeric enzyme from *Escherichia coli*. *Journal of Biological Chemistry* **273**, 5655–5661.

Bentrop, D., Bertini, I., Iacoviello, R., Luchinat, C., Niikura, Y., Piccioli, M., Presenti, C. & Rosato, A. (1999). Structural and dynamical properties of a partially unfolded Fe4S4 protein: role of the cofactor in protein folding. *Biochemistry* **38**, 4669–4680.

Bera, A. K., Grinberg, A. & Bernhardt, R. (1999). A step toward understanding the folding mechanism of bovine adrenodoxin. *Archives of Biochemistry and Biophysics* **361**, 315–322.

Berg, J. M. & Shi, Y. (1996). The galvanization of biology: a growing appreciation for the roles of zinc. *Science* **271**, 1081–1085.

Bertini, I., Cowan, J. A., Luchinat, C., Natarajan, K. & Piccioli, M. (1997). Characterization of a partially unfolded high potential iron protein. *Biochemistry* **36**, 9332–9339.

Bertini, I., Gary, H. B., Lippard, S. J. & Valentine, J. S. (1994). *Bioinorganic Chemistry*. University Science Books, Mill Valley, CA.

Bertini, I., Luchinat, C., Piccioli, M. & Soriano, A. (1998). Folding properties of iron-sulfur proteins. *Inorganica Chimica Acta* **283**, 12–16.

Betz, S., Fairman, R., O'Neil, K., Lear, J. & Degrado, W. (1995). Design of two-stranded and three-stranded coiled-coil peptides. *Philosophical Transactions of the Royal Society of London B: Biological Sciences* **348**, 81–88.

Blackledge, M. J., Guerlesquin, F. & Marion, D. (1995a). Novel methionine ligand position in cytochrome c553 and implications for sequence alignment [Letter]. *Nature Structural Biology* **2**, 532–535.

Blackledge, M. J., Guerlesquin, F. & Marion, D. (1996). Comparison of low oxidoreduction potential cytochrome c553 from *Desulfovibrio vulgaris* with the class I cytochrome c family. *Proteins* **24**, 178–914.

Blackledge, M. J., Medvedeva, S., Poncin, M., Guerlesquin, F., Bruschi, M. & Marion, D. (1995b). Structure and dynamics of ferrocytochrome c553 from *Desulfovibrio vulgaris* studied by NMR spectroscopy and restrained molecular dynamics. *Journal of Molecular Biology* **245**, 661–681.

Bryson, J. W., Betz, S. F., Lu, H. S., Suich, D. J., Zhou, H. X., O'Neil, K. T. & DeGrado, W. F. (1995). Protein design: a hierarchic approach. *Science* **270**, 935–941.

Burova, T. V., Bernhardt, R. & Pfeil, W. (1995). Conformational stability of bovine holo and apo adrenodoxin – a scanning calorimetric study. *Protein Science* **4**, 909–916.

Chan, C. K., Hofrichter, J. & Eaton, W. A. (1996). Optical triggers of protein folding. *Science* **274**, 628–629.

Chavez, L. L., Onuchic, J. N. & Clementi, C. (2004). Quantifying the roughness on the free energy landscape: entropic bottlenecks and protein folding rates. *Journal of the American Chemical Society* **126**, 8426–8432.

Chen, E., Goldbeck, R. A. & Kliger, D. S. (2004). The earliest events in protein folding: a structural requirement for ultrafast folding in cytochrome c. *Journal of the American Chemical Society* **126**, 11175–11181.

Chen, E., Wittung-Stafshede, P. & Kliger, D. (1999). Far-UV time-resolved circular dichroism detection of electron-transfer-triggered cytochrome c folding. *Journal of the American Chemical Society* **121**, 3811–3817.

Chiba, K., Ikai, A., Kawamura-Konishi, Y. & Kihara, H. (1994). Kinetic study on myoglobin refolding monitored by five optical probe stopped-flow methods. *Proteins* **19**, 110–119.

Colon, W., Wakem, L. P., Sherman, F. & Roder, H. (1997). Identification of the predominant non-native histidine ligand in unfolded cytochrome c. *Biochemistry* **36**, 12535–12541.

Dean, D. R., Bolin, J. T. & Zheng, L. (1993). Nitrogenase metalloclusters: structures, organization, and synthesis. *Journal of Bacteriology* **175**, 6737–6744.

DeBeer, S., Wittung-Stafshede, P., Leckner, J., Karlsson, G., Winkler, J. R., Gray, H. B., Malmstrom, B., Solomon, E. I., Hedman, B. & Hodgson, K. (2000). X-ray absorption spectroscopy of unfolded copper(I) azurin. *Inorganica Chimica Acta* **297**, 278–282.

DeGrado, W. F., Summa, C. M., Pavone, V., Nastri, F. & Lombardi, A. (1999). De novo design and structural characterization of proteins and metalloproteins. *Annual Review of Biochemistry* **68**, 779–819.

Dieckmann, G. R., McRorie, D. K., Lear, J. D., Sharp, K. A., DeGrado, W. F. & Pecoraro, V. L. (1998). The role of protonation and metal chelation preferences in defining the properties of mercury-binding coiled coils. *Journal of Molecular Biology* **280**, 897–912.

Dyson, H. J. & Wright, P. E. (2004). Unfolded proteins and protein folding studied by NMR. *Chemical Reviews* **104**, 3607–3622.

Engman, K. C., Sandberg, A., Leckner, J. & Karlsson, B. G. (2004). Probing the influence on folding behavior of structurally conserved core residues in *P. aeruginosa* apo-azurin. *Protein Science* **13**, 2706–2715.

Farrer, B. T. & Pecoraro, V. L. (2003). Hg(II) binding to a weakly associated coiled coil nucleates an encoded metalloprotein fold: a kinetic analysis. *Proceedings of the National Academy of Sciences USA* **100**, 3760–3765.

Feng, Y., Sligar, S. G. & Wand, A. J. (1994). Solution structure of apocytochrome b562. *Nature Structural Biology* **1**, 30–35.

Feng, Y. Q. & Sligar, S. G. (1991). Effect of heme binding on the structure and stability of *Escherichia coli* apocytochrome b562. *Biochemistry* **30**, 10150–10155.

Fenton, D. E. (1995). *Biocoordination Chemistry*. Oxford, UK: Oxford University Press.

Fersht, A. (1999). *Structure and Mechanism in Protein Science*. New York: W. H. Freeman and Company.

Fersht, A. R. (2000). Transition-state structure as a unifying basis in protein-folding mechanisms: contact order, chain topology, stability, and the extended nucleus mechanism. *Proceedings of the National Academy of Sciences USA* **97**, 1525–1529.

Filimonov, V. V., Prieto, J., Martinez, J. C., Bruix, M., Mateo, P. L. & Serrano, L. (1993). Thermodynamic analysis of the chemotactic protein from *Escherichia coli*, CheY. *Biochemistry* **32**, 12906–21.

Finn, B. E., Evenas, J., Drakenberg, T., Waltho, J. P., Thulin, E. & Forsen, S. (1995). Calcium-induced structural changes and domain autonomy in calmodulin. *Nature Structural Biology* **2**, 777–783.

Forge, V., Wijesinha, R. T., Balbach, J., Brew, K., Robinson, C. V., Redfield, C. & Dobson, C. M. (1999). Rapid collapse and slow structural reorganisation during

the refolding of bovine alpha-lactalbumin. *Journal of Molecular Biology* **288**, 673–688.

Frankel, A. D., Berg, J. M. & Pabo, C. O. (1987). Metal-dependent folding of a single zinc finger from transcription factor IIIA. *Proceedings of the National Academy of Sciences USA* **84**, 4841–4845.

Gailer, J., George, G. N., Pickering, I. J., Prince, R. C., Kohlhepp, P., Zhang, D., Walker, F. A. & Winzerling, J. J. (2001). Human cytosolic iron regulatory protein 1 contains a linear iron-sulfur cluster. *Journal of the American Chemical Society* **123**, 10121–10122.

Garcia, P., Bruix, M., Rico, M., Ciofi-Baffoni, S., Banci, L., Ramachandra Shastry, M. C., Roder, H., de Lumley Woodyear, T., Johnson, C. M., Fersht, A. R. & Barker, P. D. (2005). Effects of heme on the structure of the denatured state and folding kinetics of cytochrome b562. *Journal of Molecular Biology* **346**, 331–344.

Ghadiri, M. R. & Choi, C. (1990). Secondary structure nucleation in peptides. Transition metal ion stabilized alpha-helices. *Journal of the American Chemical Society* **112**, 1630–1632.

Ghosh, D. & Pecoraro, V. L. (2004). Understanding metalloprotein folding using a de novo design strategy. *Inorganic Chemistry* **43**, 7902–7915.

Goedken, E. R., Keck, J. L., Berger, J. M. & Marqusee, S. (2000). Divalent metal cofactor binding in the kinetic folding trajectory of *Escherichia coli* ribonuclease HI. *Protein Science* **9**, 1914–1921.

Goldman, B. S., Gabbert, K. K. & Kranz, R. G. (1996). Use of heme reporters for studies of cytochrome biosynthesis and heme transport. *Journal of Bacteriology* **178**, 6338–6347.

Gray, H. B. (2003). Biological inorganic chemistry at the beginning of the 21st century. *Proceedings of the National Academy of Sciences USA* **100**, 3563–3568.

Griffin, S., Higgins, C., Soulimane, T. & Wittung-Stafshede, P. (2003). High thermal and chemical stability of *Thermus thermophilus* seven-iron ferredoxin. *European Journal of Biochemistry* **270**, 1–8.

Guidry, J. & Wittung-Stafshede, P. (2000a). Cytochrome c(553), a small heme protein that lacks misligation in its unfolded state, folds with rapid two-state kinetics. *Journal of Molecular Biology* **301**, 769–773.

Guidry, J. & Wittung-Stafshede, P. (2000b). Stability determines formation rate of four-helix-bundle protein. *Archives of Biochemistry and Biophysics* **378**, 190–191.

Hagen, K., Watson, A. & Holm, R. (1983). Synthetic routes to iron-sulphur clusters from the common percursor [Fe(SC2H5)4]2+. *Journal of the American Chemical Society* **105**, 3905–3913.

Hagen, S. J. & Eaton, W. A. (2000). Two-state expansion and collapse of a polypeptide. *Journal of Molecular Biology* **297**, 781–789.

Hagen, S. J., Hofrichter, J., Szabo, A. & Eaton, W. A. (1996). Diffusion-limited contact formation in unfolded cytochrome c: estimating the maximum rate of protein folding [see comments]. *Proceedings of the National Academy of Sciences USA* **93**, 11615–11617.

Hammack, B., Godbole, S. & Bowler, B. E. (1998). Cytochrome c folding traps are not due solely to histidine-heme ligation: direct demonstration of a role for N-terminal amino group- heme ligation. *Journal of Molecular Biology* **275**, 719–724.

Hargrove, M. S., Krzywda, S., Wilkinson, A. J., Dou, Y., Ikeda-Saito, M. & Olson, J. S. (1994). Stability of myoglobin: a model for the folding of heme proteins. *Biochemistry* **33**, 11767–11775.

Hargrove, M. S. & Olson, J. S. (1996). The stability of holomyoglobin is determined by heme affinity. *Biochemistry* **35**, 11310–11318.

Henkens, R. W., Kitchell, B. B., Lottich, S. C., Stein, P. J. & Williams, T. J. (1982). Detection and characterization using circular dichroism and fluorescence spectroscopy of a stable intermediate conformation formed in the denaturation of bovine carbonic anhydrase with guanidinium chloride. *Biochemistry* **21**, 5918–5923.

Higgins, C. L. & Wittung-Stafshede, P. (2004). Formation of linear three-iron clusters in *Aquifex aeolicus* two-iron ferredoxins: effect of protein-unfolding speed. *Archives of Biochemistry and Biophysics* **427**, 154–163.

Hitomi, Y., Outten, C. E. & O'Halloran, T. V. (2001). Extreme zinc-binding thermodynamics of the metal sensor/regulator protein, ZntR. *Journal of the American Chemical Society* **123**, 8614–8615.

Inouye, H. & Kirschner, D. A. (1996). Refined fibril structures: the hydrophobic core in Alzheimer's amyloid beta-protein and prion as revealed by X-ray diffraction. *Ciba Foundation Symposium* **199**, 22–35; discussion 35–39.

Jackson, S. E. (1998). How do small single-domain proteins fold? *Folding & Design* **3**, R81–R91.

Jamin, M. & Baldwin, R. L. (1996). Refolding and unfolding kinetics of the equilibrium folding intermediate of apomyoglobin. *Nature Structural Biology* **3**, 613–618.

Jamin, M. & Baldwin, R. L. (1998). Two forms of the pH 4 folding intermediate of apomyoglobin. *Journal of Molecular Biology* **276**, 491–504.

Jones, C. M., Henry, E. R., Hu, Y., Chan, C. K., Luck, S. D., Bhuyan, A., Roder, H., Hofrichter, J. & Eaton, W. A. (1993). Fast events in protein folding initiated by nanosecond laser photolysis. *Proceedings of the National Academy of Sciences USA* **90**, 11860–11864.

Jones, K., Gomes, C. M., Huber, H., Teixeira, M. & Wittung-Stafshede, P. (2002). Formation of a linear [3Fe-4S] cluster in a seven-iron ferredoxin triggered by polypeptide unfolding. *Journal of Biological Inorganic Chemistry* **7**, 357–362.

Kamagata, K., Arai, M. & Kuwajima, K. (2004). Unification of the folding mechanisms of non-two-state and two-state proteins. *Journal of Molecular Biology* **339**, 951–965.

KENNEDY, M. C., KENT, T. A., EMPTAGE, M., MERKLE, H., BEINERT, H. & MUNCK, E. (1984). Evidence for the formation of a linear [3Fe-4S] cluster in partially unfolded aconitase. *Journal of Biological Chemistry* **259**, 14463–14471.

KISTER, A. E., FINKELSTEIN, A. V. & GELFAND, I. M. (2002). Common features in structures and sequences of sandwich-like proteins. *Proceedings of the National Academy of Sciences USA* **99**, 14137–14141.

KIYOKAWA, T., KANAORI, K., TAJIMA, K., KOIKE, M., MIZUNO, T., OKU, J. I. & TANAKA, T. (2004). Binding of Cu(II) or Zn(II) in a de novo designed triple-stranded alpha-helical coiled-coil toward a prototype for a metalloenzyme. *Journal of Peptide Research* **63**, 347–353.

KLUG, A. & SCHWABE, J. W. (1995). Protein motifs 5. Zinc fingers. *FASEB Journal* **9**, 597–604.

KOHN, W. D., KAY, C. M. & HODGES, R. S. (1998a). Effects of lanthanide binding on the stability of de novo designed alpha-helical coiled-coils. *Journal of Peptide Research* **51**, 9–18.

KOHN, W. D., KAY, C. M. & HODGES, R. S. (1998b). Orientation, positional, additivity, and oligomerization-state effects of interhelical ion pairs in alpha-helical coiled-coils. *Journal of Molecular Biology* **283**, 993–1012.

KUBONIWA, H., TJANDRA, N., GRZESIEK, S., REN, H., KLEE, C. B. & BAX, A. (1995). Solution structure of calcium-free calmodulin. *Nature Structural Biology* **2**, 768–776.

KUWAJIMA, K., MITANI, M. & SUGAI, S. (1989). Characterization of the critical state in protein folding. Effects of guanidine hydrochloride and specific Ca^{2+} binding on the folding kinetics of alpha-lactalbumin. *Journal of Molecular Biology* **206**, 547–561.

LACHENMANN, M. J., LADBURY, J. E., DONG, J., HUANG, K., CAREY, P. & WEISS, M. A. (2004). Why zinc fingers prefer zinc: ligand-field symmetry and the hidden thermodynamics of metal ion selectivity. *Biochemistry* **43**, 13910–13925.

LAMB, A. L., TORRES, A. S., O'HALLORAN, T. V. & ROSENZWEIG, A. C. (2001). Heterodimeric structure of superoxide dismutase in complex with its metallochaperone. *Nature Structural Biology* **8**, 751–755.

LAMB, A. L., WERNIMONT, A. K., PUFAHL, R. A., CULOTTA, V. C., O'HALLORAN, T. V. & ROSENZWEIG, A. C. (1999). Crystal structure of the copper chaperone for superoxide dismutase. *Nature Structural Biology* **6**, 724–729.

LANSBURY JR., P. T., COSTA, P. R., GRIFFITHS, J. M., SIMON, E. J., AUGER, M., HALVERSON, K. J., KOCISKO, D. A., HENDSCH, Z. S., ASHBURN, T. T., SPENCER, R. G., TIDOR, B. & GRIFFIN, R. G. (1995). Structural model for the beta-amyloid fibril based on interstrand alignment of an antiparallel-sheet comprising a C-terminal peptide. *Nature Structural Biology* **2**, 990–998.

LEAL, S. S., TEIXEIRA, M. & GOMES, C. M. (2004). Studies on the degradation pathway of iron-sulfur centers during unfolding of a hyperstable ferredoxin: cluster dissociation, iron release and protein stability. *Journal of Biological Inorganic Chemistry* **9**, 987–996.

LECKNER, J., BONANDER, N., WITTUNG-STAFSHEDE, P., MALMSTROM, B. G. & KARLSSON, B. G. (1997a). The effect of the metal ion on the folding energetics of azurin: a comparison of the native, zinc and apoprotein. *Biochimica et Biophysica Acta* **1342**, 19–27.

LECKNER, J., WITTUNG, P., BONANDER, N., KARLSSON, G. & MALMSTROM, B. (1997b). The effect of redox state on the folding free energy of azurin. *Journal of Biological Inorganic Chemistry* **2**, 368–371.

LINDORFF-LARSEN, K., VENDRUSCOLO, M., PACI, E. & DOBSON, C. M. (2004). Transition states for protein folding have native topologies despite high structural variability. *Natural Structure & Molecular Biology* **11**, 443–449.

LIPPARD, S. J. & BERG, J. M. (1994). *Principles of Bioinorganic Chemistry*. University Science Books, Mill Valley, CA.

LOVELL, M. A., ROBERTSON, J. D., TEESDALE, W. J., CAMPBELL, J. L. & MARKESBERY, W. R. (1998). Copper, iron and zinc in Alzheimer's disease senile plaques. *Journal of the Neurological Sciences* **158**, 47–52.

LUISI, D. L., WU, W. J. & RALEIGH, D. P. (1999). Conformational analysis of a set of peptides corresponding to the entire primary sequence of the N-terminal domain of the ribosomal protein L9: evidence for stable native-like secondary structure in the unfolded state. *Journal of Molecular Biology* **287**, 395–407.

MAKAROV, D. E. & PLAXCO, K. W. (2003). The topomer search model: a simple, quantitative theory of two-state protein folding kinetics. *Protein Science* **12**, 17–26.

MANDAL, S., DAS, G., SINGH, R., SHUKLA, R. & BHARADWAJ, P. K. (1997). Synthesis and studies of Cu(II)-thiolato complexes: Bioinorganic perspectives. *Coordination Chemistry Reviews* **160**, 191–235.

MANYUSA, S., MORTUZA, G. & WHITFORD, D. (1999). Analysis of folding and unfolding reactions of cytochrome b5. *Biochemistry* **38**, 14352–14362.

MANYUSA, S. & WHITFORD, D. (1999). Defining folding and unfolding reactions of apocytochrome b5 using equilibrium and kinetic fluorescence measurements. *Biochemistry* **38**, 9533–9540.

MARET, W. & VALLEE, B. L. (1993). Cobalt as probe and label of proteins. *Methods in Enzymology* **226**, 52–71.

MARKS, J., POZDNYAKOVA, I., GUIDRY, J. & WITTUNG-STAFSHEDE, P. (2004). Methionine-121 coordination determines metal specificity in unfolded *Pseudomonas aeruginosa* azurin. *Journal of Biological Inorganic Chemistry* **9**, 281–288.

MASINO, L., MARTIN, S. R. & BAYLEY, P. M. (2000). Ligand binding and thermodynamic stability of a multidomain protein, calmodulin. *Protein Science* **9**, 1519–1529.

MASTERS, C. L., SIMMS, G., WEINMAN, N. A., MULTHAUP, G., MCDONALD, B. L. & BEYREUTHER, K. (1985). Amyloid plaque core protein in Alzheimer disease and

Down syndrome. *Proceedings of the National Academy of Sciences USA* **82**, 4245–4249.

Matouschek, A. & Fersht, A. R. (1991). Protein engineering in analysis of protein folding pathways and stability. *Methods in Enzymology* **202**, 82–112.

Matouschek, A., Kellis Jr., J. T., Serrano, L., Bycroft, M. & Fersht, A. R. (1990). Transient folding intermediates characterized by protein engineering. *Nature* **346**, 440–445.

Matthews, C. R. (1993). Pathways of protein folding. *Annual Review of Biochemistry* **62**, 653–683.

Matthews, J. M. & Sunde, M. (2002). Zinc fingers – folds for many occasions. *IUBMB Life* **54**, 351–355.

Mei, G., Rosato, N., Silva Jr., N., Rusch, R., Gratton, E., Savini, I. & Finazzi-Agro, A. (1992). Denaturation of human Cu/Zn superoxide dismutase by guanidine hydrochloride: a dynamic fluorescence study. *Biochemistry* **31**, 7224–7230.

Mines, G. A., Pascher, T., Lee, S. C., Winkler, J. R. & Gray, H. B. (1996). Cytochrome c folding triggered by electron transfer. *Chemical Biology* **3**, 491–497.

Miura, T., Satoh, T. & Takeuchi, H. (1998). Role of metal-ligand coordination in the folding pathway of zinc finger peptides. *Biochimica et Biophysica Acta* **1384**, 171–179.

Miura, T., Suzuki, K., Kohata, N. & Takeuchi, H. (2000). Metal binding modes of Alzheimer's amyloid beta-peptide in insoluble aggregates and soluble complexes. *Biochemistry* **39**, 7024–7031.

Moczygemba, C., Guidry, J., Jones, K. L., Gomes, C. M., Teixeira, M. & Wittung-Stafshede, P. (2001). High stability of a ferredoxin from the hyperthermophilic archaeon *A. ambivalens*: involvement of electrostatic interactions and cofactors. *Protein Science* **10**, 1539–1548.

Moczygemba, C., Guidry, J. & Wittung-Stafshede, P. (2000). Heme orientation affects holo-myoglobin folding and unfolding kinetics. *FEBS Letters* **470**, 203–206.

Muller, F. (1992). *Chemistry and Biochemistry of Flavoenzymes*. Boca Raton, FL: CRC Press.

Nar, H., Huber, R., Messerschmidt, A., Filippou, A. C., Barth, M., Jaquinod, M., van de Kamp, M. & Canters, G. W. (1992a). Characterization and crystal structure of zinc azurin, a by-product of heterologous expression in *Escherichia coli* of *Pseudomonas aeruginosa* copper azurin. *European Journal of Biochemistry* **205**, 1123–1129.

Nar, H., Messerschmidt, A., Huber, R., van de Kamp, M. & Canters, G. W. (1991). Crystal structure analysis of oxidized *Pseudomonas aeruginosa* azurin at pH 5·5 and pH 9·0. A pH-induced conformational transition involves a peptide bond flip. *Journal of Molecular Biology* **221**, 765–772.

Nar, H., Messerschmidt, A., Huber, R., van de Kamp, M. & Canters, G. W. (1992b). Crystal structure of *Pseudomonas aeruginosa* apo-azurin at 1·85 A resolution. *FEBS Letters* **306**, 119–124.

O'Halloran, T. V. & Culotta, V. C. (2000). Metallochaperones, an intracellular shuttle service for metal ions. *Journal of Biological Chemistry* **275**, 25057–25060.

O'Neil, K. T. & DeGrado, W. F. (1990). A thermodynamic scale for the helix-forming tendencies of the commonly occurring amino acids. *Science* **250**, 646–651.

Oliveberg, M. (2001). Characterisation of the transition states for protein folding: towards a new level of mechanistic detail in protein engineering analysis. *Current Opinion in Structural Biology* **11**, 94–100.

Oliveberg, M., Tan, Y. J., Silow, M. & Fersht, A. R. (1998). The changing nature of the protein folding transition state: implications for the shape of the free-energy profile for folding. *Journal of Molecular Biology* **277**, 933–943.

Ollagnier-De Choudens, S., Mattioli, T., Takahashi, Y. & Fontecave, M. (2001). Iron-sulfur cluster assembly: characterization of IscA and evidence for a specific and functional complex with ferredoxin. *Journal of Biological Chemistry* **276**, 22604–22607.

Ollagnier-De Choudens, S., Sanakis, Y., Hewitson, K. S., Roach, P., Baldwin, J. E., Munck, E. & Fontecave, M. (2000). Iron-sulfur center of biotin synthase and lipoate synthase. *Biochemistry* **39**, 4165–4173.

Otzen, D. E., Kristensen, O., Proctor, M. & Oliveberg, M. (1999). Structural changes in the transition state of protein folding: alternative interpretations of curved chevron plots. *Biochemistry* **38**, 6499–6511.

Outten, C. E. & O'Halloran, T. V. (2001). Femtomolar sensitivity of metalloregulatory proteins controlling zinc homeostasis. *Science* **292**, 2488–2492.

Pagani, S., Vecchio, G., Iametti, S., Bianchi, R. & Bonomi, F. (1986). On the role of 2Fe-2S cluster in the formation of the structure of spinach ferredoxin. *Biochimica et Biophysica Acta* **870**, 538–544.

Parraga, G., Horvath, S., Hood, L., Young, E. T. & Klevit, R. E. (1990). Spectroscopic studies of wild-type and mutant 'zinc finger' peptides: determinants of domain folding and structure. *Proceedings of the National Academy of Sciences USA* **87**, 137–41.

Patzer, S. I. & Hantke, K. (1998). The ZnuABC high-affinity zinc uptake system and its regulator Zur in *Escherichia coli*. *Molecular Microbiology* **28**, 1199–1210.

Petkova, A. T., Ishii, Y., Balbach, J. J., Antzutkin, O. N., Leapman, R. D., Delaglio, F. & Tycko, R. (2002). A structural model for Alzheimer's beta-amyloid fibrils based on experimental constraints from solid state NMR. *Proceedings of the National Academy of Sciences USA* **99**, 16742–16747.

Pierce, M. M. & Nall, B. T. (1997). Fast folding of cytochrome c. *Protein Science* **6**, 618–627.

Plaxco, K. W., Simons, K. T. & Baker, D. (1998). Contact order, transition state placement and the refolding rates of single domain proteins. *Journal of Molecular Biology* **277**, 985–994.

Plaxco, K. W., Simons, K. T., Ruczinski, I. & David, B. (2000). Topology, stability, sequence, and length: Defining the determinants of two-state protein folding kinetics. *Biochemistry* **39**, 11177–11183.

Pozdnyakova, I., Guidry, J. & Wittung-Stafshede, P. (2000). Copper triggered b-hairpin formation. Initiation site for azurin folding? *Journal of the American Chemical Society* **122**, 6337–6338.

Pozdnyakova, I., Guidry, J. & Wittung-Stafshede, P. (2001a). Copper stabilizes azurin by decreasing the unfolding rate. *Archives of Biochemistry and Biophysics* **390**, 146–148.

Pozdnyakova, I., Guidry, J. & Wittung-Stafshede, P. (2001b). Probing copper ligands in denatured Pseudomonas aeruginosa azurin: unfolding His117Gly and His46Gly mutants. *Journal of Biological Inorganic Chemistry* **6**, 182–188.

Pozdnyakova, I., Guidry, J. & Wittung-Stafshede, P. (2002). Studies of *Pseudomonas aeruginosa* azurin mutants: cavities in beta-barrel do not affect refolding speed. *Biophysical Journal* **82**, 2645–2651.

Pozdnyakova, I. & Wittung-Stafshede, P. (2001a). Biological relevance of metal binding before protein folding. *Journal of the American Chemical Society* **123**, 10135–10136.

Pozdnyakova, I. & Wittung-Stafshede, P. (2001b). Copper binding before polypeptide folding speeds up formation of active (holo) *Pseudomonas aeruginosa* azurin. *Biochemistry* **40**, 13728–13733.

Pozdnyakova, I. & Wittung-Stafshede, P. (2003). Approaching the speed limit for Greek Key beta-barrel formation: transition-state movement tunes folding rate of zinc-substituted azurin. *Biochimica Biophysica Acta* **1651**, 1–4.

Privalov, P. L. (1996). Intermediate states in protein folding. *Journal of Molecular Biology* **258**, 707–725.

Rae, T. D., Schmidt, P. J., Pufahl, R. A., Culotta, V. C. & O'Halloran, T. V. (1999). Undetectable intracellular free copper: the requirement of a copper chaperone for superoxide dismutase. *Science* **284**, 805–808.

Raman, B., Ban, T., Yamaguchi, K. I., Sakai, M., Kawai, T., Naiki, H. & Goto, Y. (2005). Metal ion-dependent effects of clioquinol on the fibril growth of an amyloid beta peptide. *Journal of Biological Chemistry* **280**, 16157–16162.

Ramseier, T. M., Winteler, H. V. & Hennecke, H. (1991). Discovery and sequence analysis of bacterial genes involved in the biogenesis of c-type cytochromes. *Journal of Biological Chemistry* **266**, 7793–7803.

Robinson, C. R., Liu, Y., O'Brien, R., Sligar, S. G. & Sturtevant, J. M. (1998). A differential scanning calorimetric study of the thermal unfolding of apo- and holo-cytochrome b562. *Protein Science* **7**, 961–965.

Robinson, C. R., Liu, Y., Thomson, J. A., Sturtevant, J. M. & Sligar, S. G. (1997). Energetics of heme binding to native and denatured states of cytochrome b562. *Biochemistry* **36**, 16141–16146.

Roder, H. & Colon, W. (1997). Kinetic role of early intermediates in protein folding. *Current Opinion in Structural Biology* **7**, 15–28.

Sanchez, I. E. & Kiefhaber, T. (2003). Evidence for sequential barriers and obligatory intermediates in apparent two-state protein folding. *Journal of Molecular Biology* **325**, 367–376.

Scott, R. & Mauk, A. (1996). *Cytochrome c: A Multidisciplinary Approach*. Sausalito, CA: University Science Books.

Selkoe, D. J., Abraham, C. R., Podlisny, M. B. & Duffy, L. K. (1986). Isolation of low-molecular-weight proteins from amyloid plaque fibers in Alzheimer's disease. *Journal of Neurochemistry* **46**, 1820–1834.

Sola, M., Lopez-Hernandez, E., Cronet, P., Lacroix, E., Serrano, L., Coll, M. & Parraga, A. (2000). Towards understanding a molecular switch mechanism: thermodynamic and crystallographic studies of the signal transduction protein CheY. *Journal of Molecular Biology* **303**, 213–225.

Solioz, M. & Stoyanov, J. V. (2003). Copper homeostasis in *Enterococcus hirae*. *FEMS Microbiology Reviews* **27**, 183–195.

Sosnick, T. R., Mayne, L., Hiller, R. & Englander, S. W. (1994). The barriers in protein folding. *Nature Structural Biology* **1**, 149–156.

Spatz, L. & Strittmatter, P. (1971). A form of cytochrome b5 that contains an additional hydrophobic sequence of 40 amino acid residues. *Proceedings of the National Academy of Sciences USA* **68**, 1042–1046.

States, D. J., Creighton, T. E., Dobson, C. M. & Karplus, M. (1987). Conformations of intermediates in the folding of the pancreatic trypsin inhibitor. *Journal of Molecular Biology* **195**, 731–739.

Sugawara, T., Kuwajima, K. & Sugai, S. (1991). Folding of staphylococcal nuclease A studied by equilibrium and kinetic circular dichroism spectra. *Biochemistry* **30**, 2698–2706.

Suzuki, K., Hiroaki, H., Kohda, D. & Tanaka, T. (1998). An isoleucine zipper peptide forms a native-like triple stranded coiled coil in solution. *Protein Engineering* **11**, 1051–1055.

Syme, C. D., Nadal, R. C., Rigby, S. E. & Viles, J. H. (2004). Copper binding to the amyloid-beta (Abeta) peptide associated with Alzheimer's disease: folding, coordination geometry, pH dependence, stoichiometry, and affinity of Abeta-(1–28): insights from a range of complementary spectroscopic techniques. *Journal of Biological Chemistry* **279**, 18169–18177.

Tainer, J. A., Getzoff, E. D., Richardson, J. S. & Richardson, D. C. (1983). Structure and mechanism of copper, zinc superoxide dismutase. *Nature* **306**, 284–287.

Telford, J. R., Tezcan, F. A., Gray, H. B. & Winkler, J. R. (1999). Role of ligand substitution in ferrocytochrome c folding. *Biochemistry* **38**, 1944–1949.

Ternstrom, T., Mayor, U., Akke, M. & Oliveberg, M. (1999). From snapshot to movie: phi analysis of protein folding transition states taken one step further. *Proceedings of the National Academy of Sciences USA* **96**, 14854–14859.

Tjernberg, L. O., Callaway, D. J., Tjernberg, A., Hahne, S., Lilliehook, C., Terenius, L., Thyberg, J. & Nordstedt, C. (1999). A molecular model of Alzheimer amyloid beta-peptide fibril formation. *Journal of Biological Chemistry* **274**, 12619–12625.

Uzawa, T., Akiyama, S., Kimura, T., Takahashi, S., Ishimori, K., Morishima, I. & Fujisawa, T. (2004). Collapse and search dynamics of apomyoglobin folding revealed by submillisecond observations of alpha-helical content and compactness. *Proceedings of the National Academy of Sciences USA* **101**, 1171–1176.

Vijgenboom, E., Busch, J. E. & Canters, G. W. (1997). In vivo studies disprove an obligatory role of azurin in denitrification in *Pseudomonas aeruginosa* and show that azu expression is under control of rpoS and ANR. *Microbiology* **143**, 2853–2863.

Villanueva, J., Hoshino, M., Katou, H., Kardos, J., Hasegawa, K., Naiki, H. & Goto, Y. (2004). Increase in the conformational flexibility of beta 2-microglobulin upon copper binding: a possible role for copper in dialysis-related amyloidosis. *Protein Science* **13**, 797–809.

Wilson, C. J. & Wittung-Stafshede, P. (2005a). Role of structural determinants in folding of the sandwich-like protein *Pseudomonas aeruginosa* azurin. *Proceedings of the National Academy of Sciences USA* **102**, 3984–3987.

Wilson, C. J. & Wittung-Stafshede, P. (2005b). Snapshots of a dynamic folding nucleus in zinc-substituted *Pseudomonas aeruginosa* azurin. *Biochemistry* **44**, 10054–10062.

Wittung-Stafshede, P. (1999). Equilibrium unfolding of a small low-potential cytochrome, cytochrome c553 from *Desulfovibrio vulgaris*. *Protein Science* **8**, 1523–1529.

Wittung-Stafshede, P. (2002). Role of cofactors in protein folding. *Accounts of Chemical Research* **35**, 201–208.

Wittung-Stafshede, P., Hill, M. G., Gomez, E., Di Bilio, A., Karlsson, G., Leckner, J., Winkler, J. R., Gray, H. B. & Malmstrom, B. G. (1998a). Reduction potentials of blue and purple copper proteins in their unfolded states: a closer lock at rack-induced coordination. *Journal of Biological Inorganic Chemistry* **3**, 367–370.

Wittung-Stafshede, P., Lee, J. C., Winkler, J. R. & Gray, H. B. (1999). Cytochrome b562 folding triggered by electron transfer: approaching the speed limit for formation of a four-helix-bundle protein. *Proceedings of the National Academy of Sciences USA* **96**, 6587–6590.

Wittung-Stafshede, P., Malmstrom, B. G., Winkler, J. R. & Gray, H. B. (1998b). Electron-transfer triggered folding of deoxymyoglobin. *Journal of Physical Chemistry* **102**, 5599–5601.

Wolfe, S. A., Nekludova, L. & Pabo, C. O. (2000). DNA recognition by Cys2His2 zinc finger proteins. *Annual Review of Biophysics and Biomolecular Structure* **29**, 183–212.

Wong, K. P. & Hamlin, L. M. (1975). The role of Zn(II) on the folding of bovine carbonic anhydrase B. *Archives of Biochemistry and Biophysics* **170**, 12–22.

Yamada, T., Goto, M., Punj, V., Zaborina, O., Chen, M. L., Kimbara, K., Majumdar, D., Cunningham, E., Das Gupta, T. K. & Chakrabarty, A. M. (2002). Bacterial redox protein azurin, tumor suppressor protein p53, and regression of cancer. *Proceedings of the National Academy of Sciences USA* **99**, 14098–14103.

Yazgan, A. & Henkens, R. W. (1972). Role of zinc (II) in the refolding of guanidine hydrochloride denatured bovine carbonic anhydrase. *Biochemistry* **11**, 1314–1318.

Yeh, S. R. & Rousseau, D. L. (2000). Hierarchical folding of cytochrome c. *Nature Structural Biology* **7**, 443–445.

Yeh, S. R., Takahashi, S., Fan, B. & Rousseau, D. L. (1997). Ligand exchange during cytochrome c folding. *Nature Structural Biology* **4**, 51–56.

Zheng, L., White, R. H., Cash, V. L., Jack, R. F. & Dean, D. R. (1993). Cysteine desulfurase activity indicates a role for NIFS in metallocluster biosynthesis. *Proceedings of the National Academy of Sciences USA* **90**, 2754–2758.